Three-dimensional magnetotelluric modeling including topography/bathymetry

Yoshiya Usui

Earthquake Research Institute,

The University of Tokyo

Agenda

1. Influences of topography and bathymetry on MT response functions
2. Review of the methods for incorporating topography and bathymetry in 3-D MT modeling
3. Brief introduction of 3-D MT inversion code FEMTIC

Agenda

1. Influences of topography and bathymetry on MT response functions

2. Review of the methods for incorporating topography and bathymetry in 3-D MT modeling

3. Brief introduction of 3-D MT inversion code FEMTIC

Analytical MT response functions for a 2-D sinusoidal topography

The main scope of this presentation is effects of 3-D topography.

However, first, I introduce the effects of 2-D sinusoidal topography.

That is because

- We can obtain an analytical solution for 2-D sinusoidal topography
- Knowledge about 2-D topography effects is quite useful for inferring effects of 3-D topography.

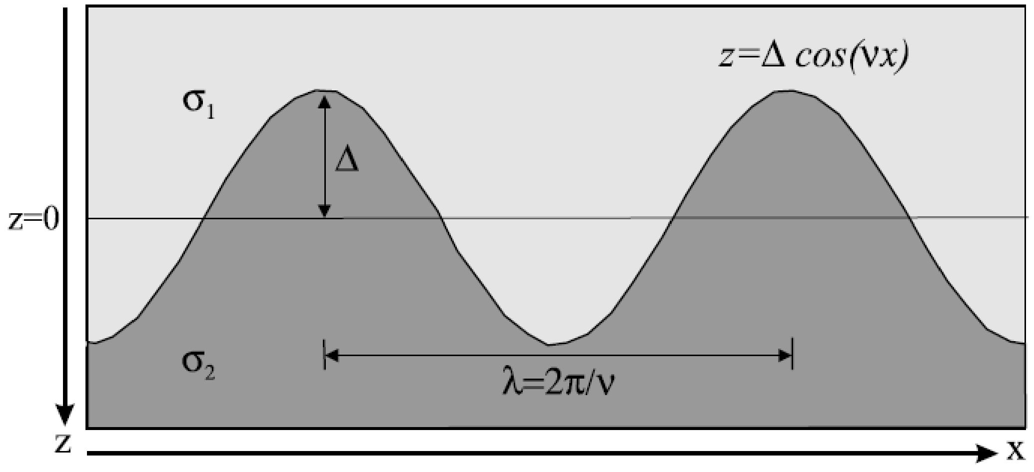

Schwalenberg & Edwards (2004, *GJI*)

- ➢ Schwalenberg & Edwards (2004, *GJI*) and Usui *et al*. (2018 , *GJI*) developed an analytical formulation for 2-D sinusoidal topography and bathymetry.
- ➢ Originally, Schwalenberg & Edwards (2004 , *GJI*) proposed the formulation.
- ➢ Later, Usui *et al*. (2018 , *GJI*) slightly modified the formulation for the TM-mode.
- ➢ In our formulation, the tangential component of the electric field, instead of the horizontal component, is continuous across the earth's surface. That satisfies the physical law of the electric field.

Spatial distribution of MT response functions for a 2-D sinusoidal land topography (1)

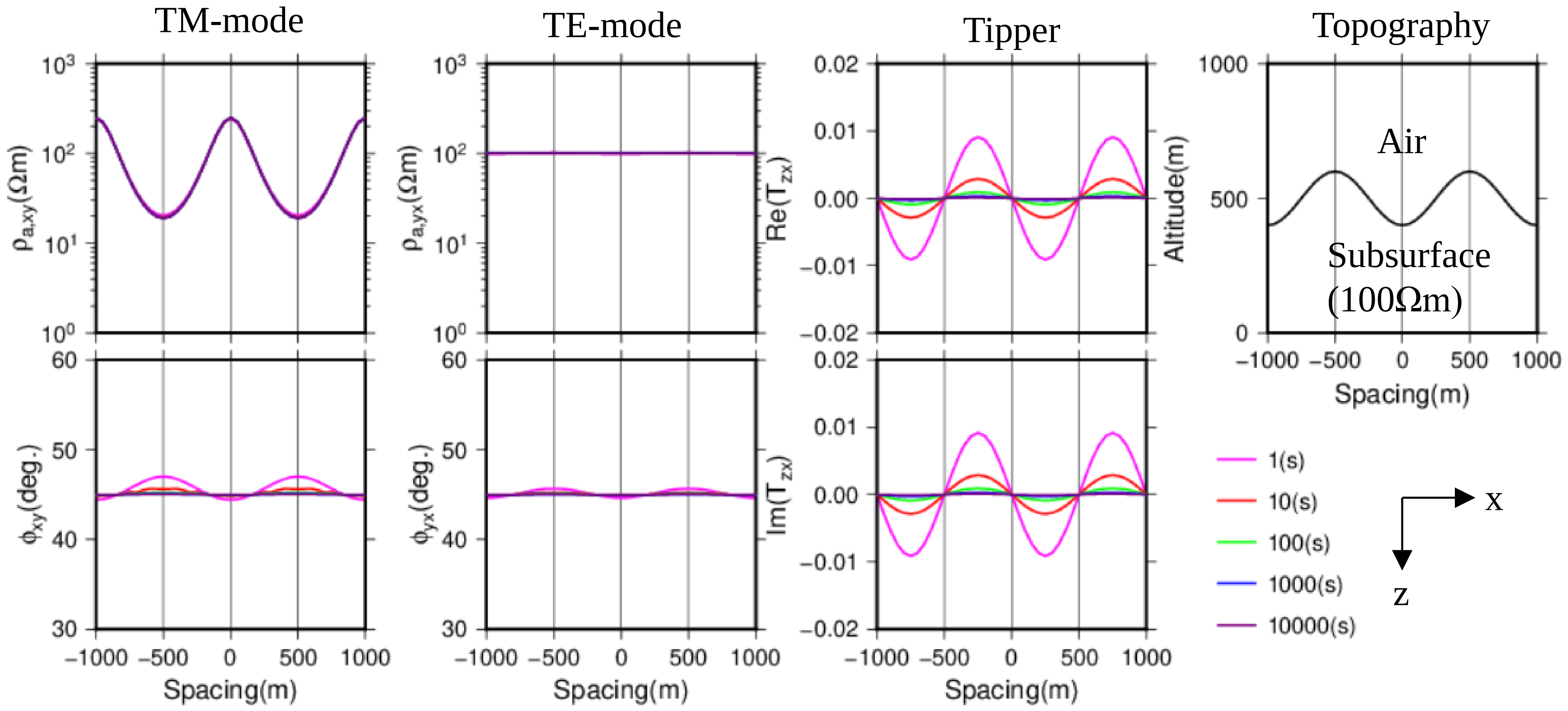

- MT response functions for different periods with a fixed subsurface resistivity (100 Ωm).
- Nearly galvanic topographic effect can be found for the TM-mode.
- Topography effects on the TE-mode response functions are relatively small.
- Topography effect on tipper increases with decreasing period. The induction arrows (Parkinson convention) point toward tops of the undulations.

Current streamlines for a 2-D sinusoidal land topography

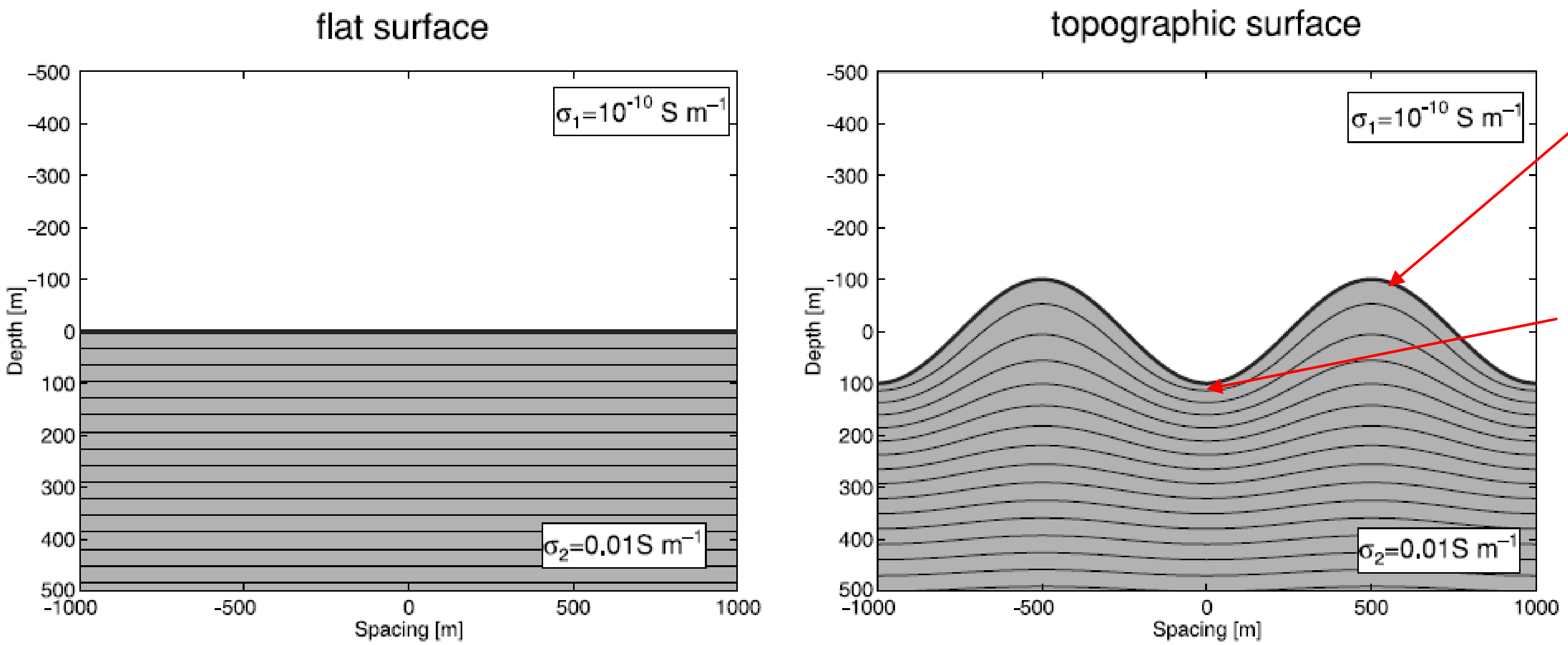

Electric current density decreases on hills
→ Apparent resistivity decreases on hills.

Electric current density increases on valleys,
→Apparent resistivity increases on valleys.

Streamlines of the electric current density
(Schwalenberg & Edwards 2004, *GJI*)

TM-mode

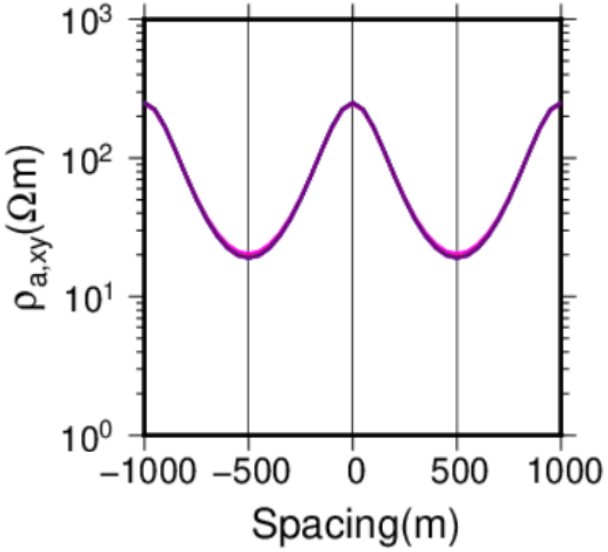

Spatial distribution of MT response functions for a 2-D sinusoidal land topography (2)

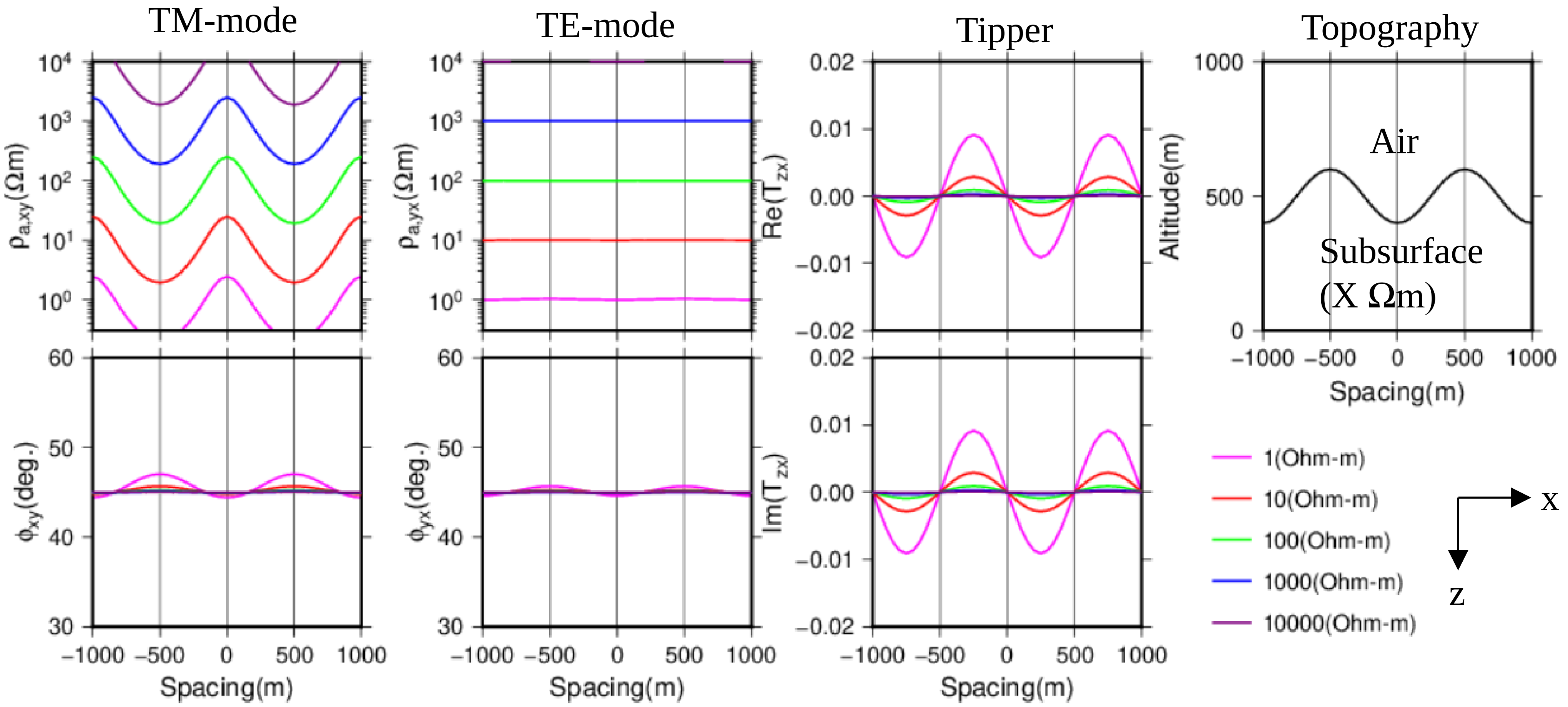

- MT response functions for different land resistivity with a fixed period (100 sec).
- Topography effects on the apparent resistivity are nearly independent of the subsurface resistivity.
- Topography effects on tipper increase with decreasing land resistivity.

Sounding curves for a 2-D sinusoidal land topography (1)

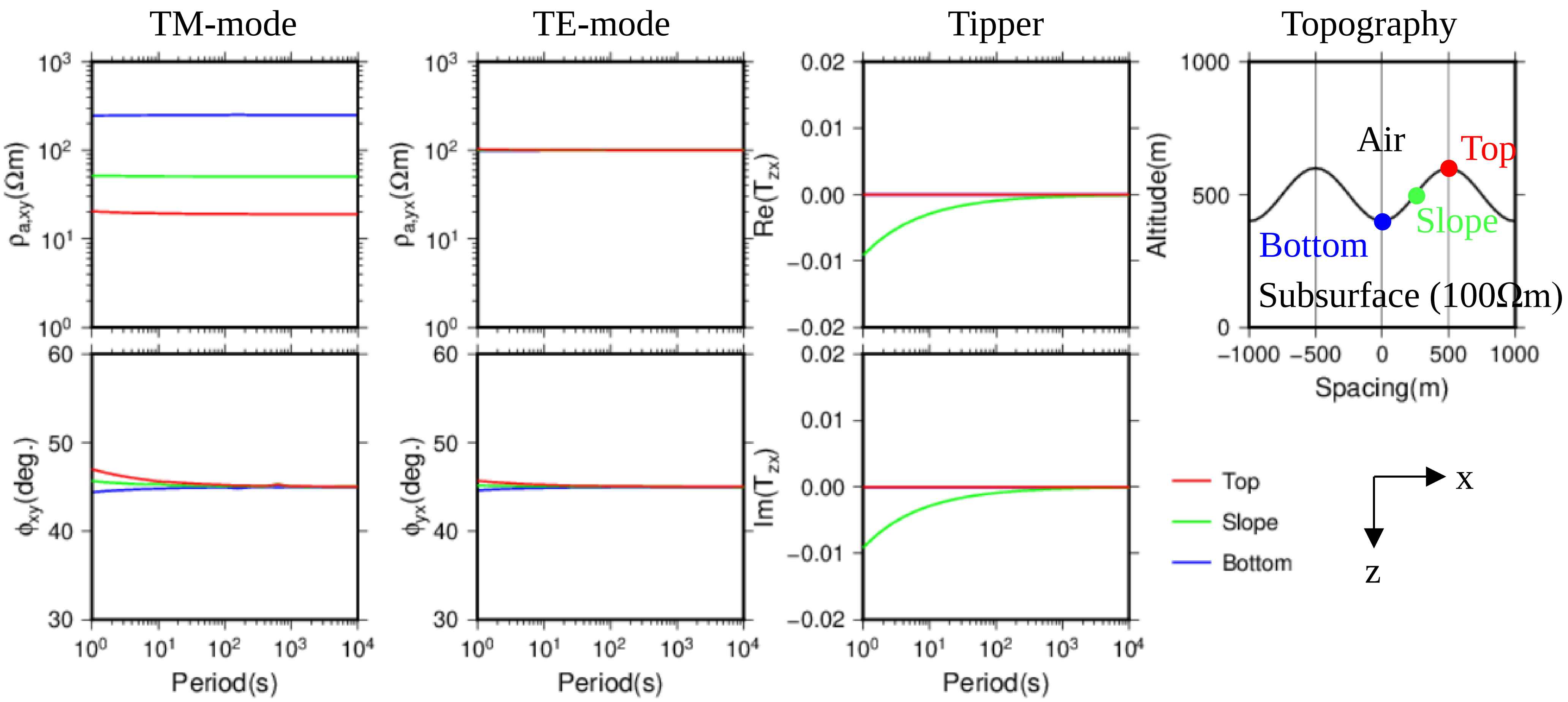

- Sounding curves on the top, slope, and bottom of the undulation are shown.
- At longer periods (> 100 s), topography effects are nearly galvanic.
- Inductive topography effects increases with decreasing period.
- Magnitude of tipper increases with decreasing period.

Sounding curves for a 2-D sinusoidal land topography (2)

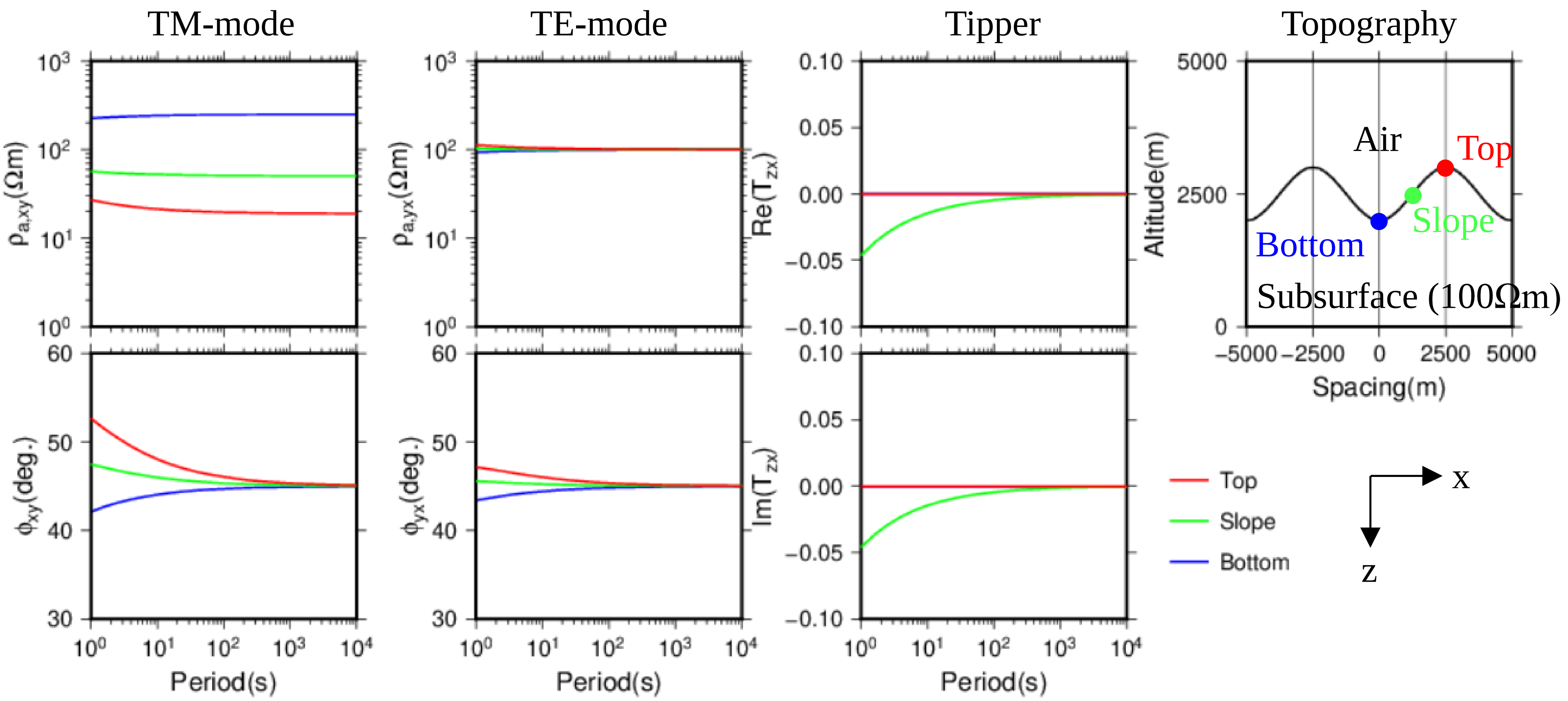

- Scale of undulation (amplitude and wavelength) is five times as large as that of the previous case.
- Inductive topography effects become large compared to the previous case.
- Topography effect depends on the scale of the undulations.
- Strength of inductive topography effects depends on the skin depth compared to the scale of undulation.

Spatial distribution of MT response functions for a 2-D sinusoidal bathymetry (1)

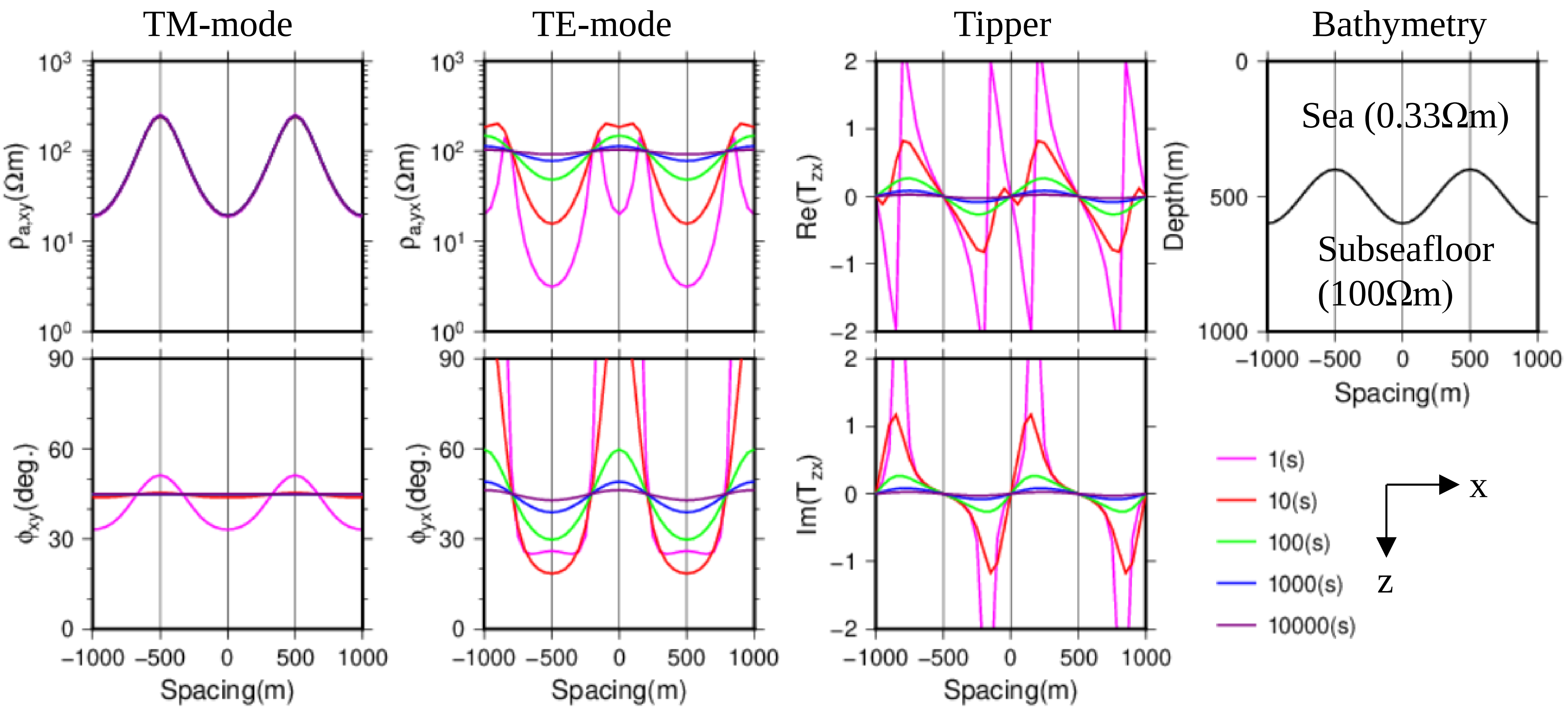

- Bathymetry effects on the TM-mode responses are nearly galvanic except for the shortest period (1 sec).
- A large difference from the land topography case is prominent bathymetry effects in the TE-mode responses functions.
- Bathymetry effects on tipper are quite large compared to land topography case.
- The induction arrows (Parkinson convention) point away from tops of the undulations.

Current streamlines for a sinusoidal bathymetry

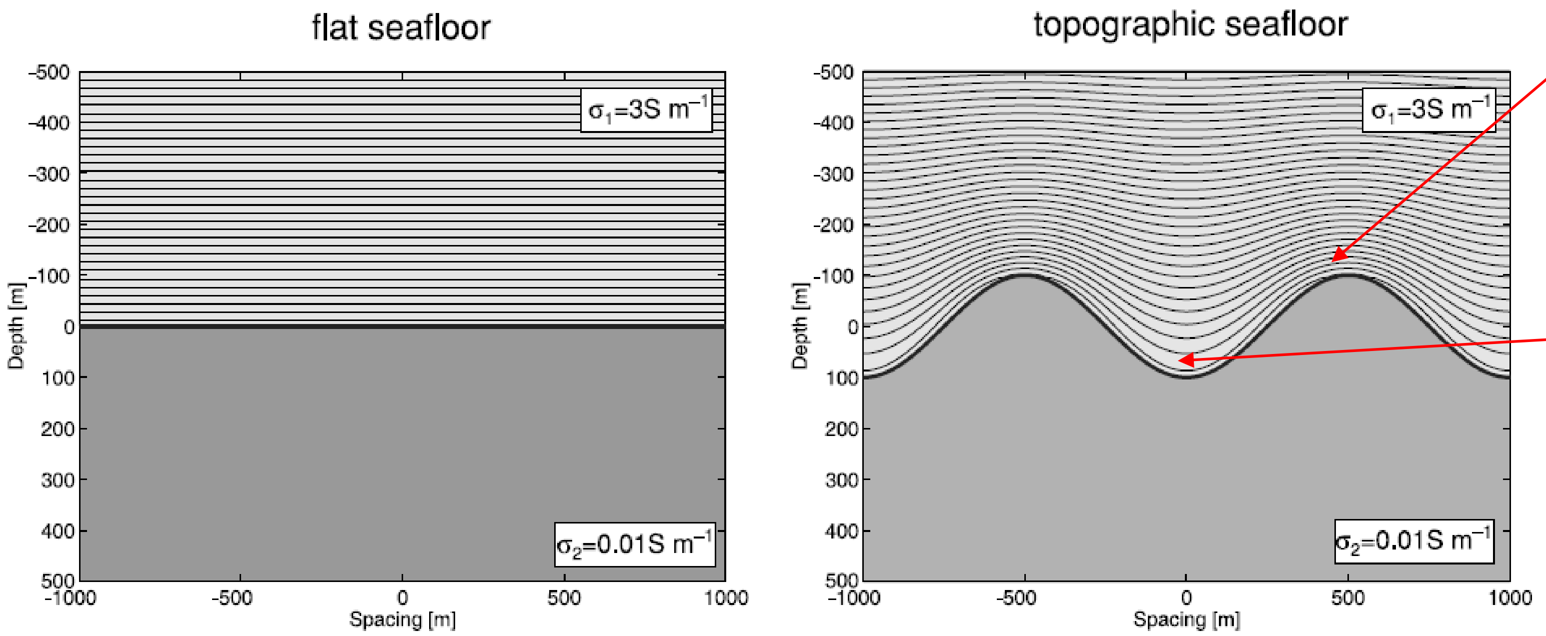

Electric current density increases on submarine hills.
→ Apparent resistivity increases on submarine hills.

Electric current density decreases on submarine valleys.
→ Apparent resistivity decreases on submarine valleys.

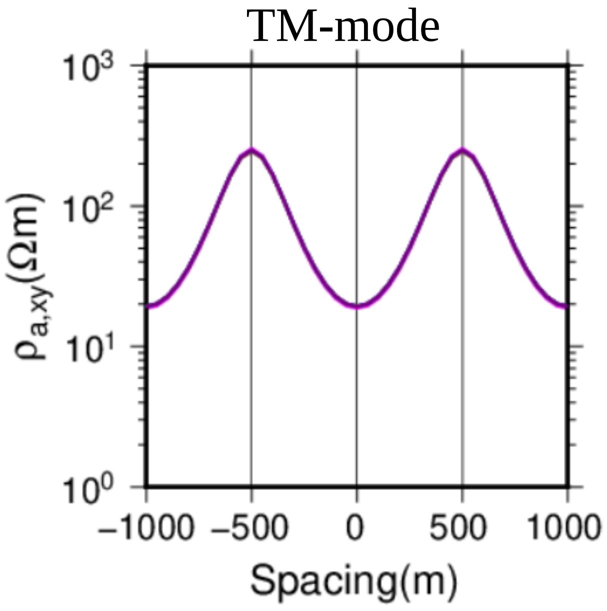

Streamlines of the electric current density
(Schwalenberg & Edwards 2004, *GJI*)

These trends are opposite to those of the land topography case.

Electromagnetic field of the TE-mode

Absolute values of the electric field

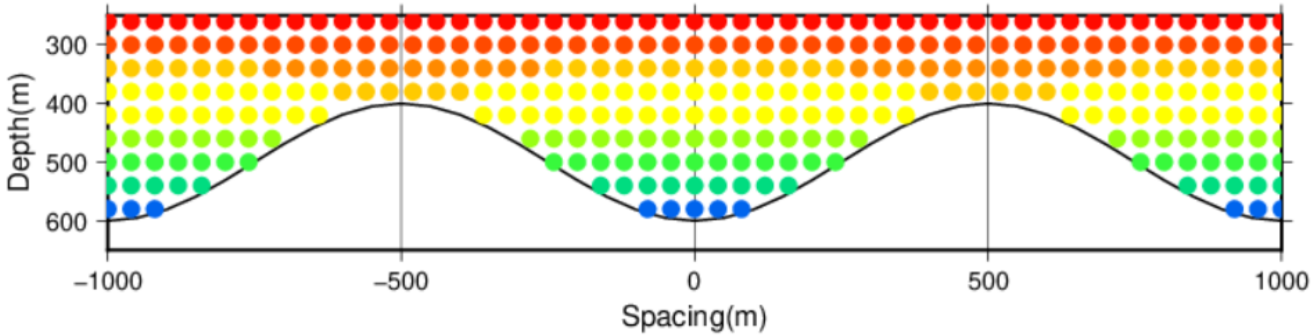

Real components of the magnetic field vectors

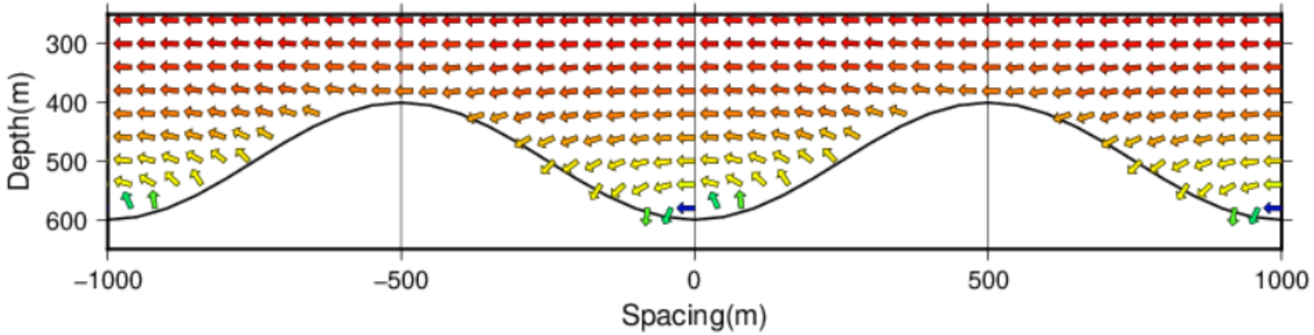

Time-averages of the complex Poynting vectors: $0.5Re(\boldsymbol{E} \times \boldsymbol{H}^*)$

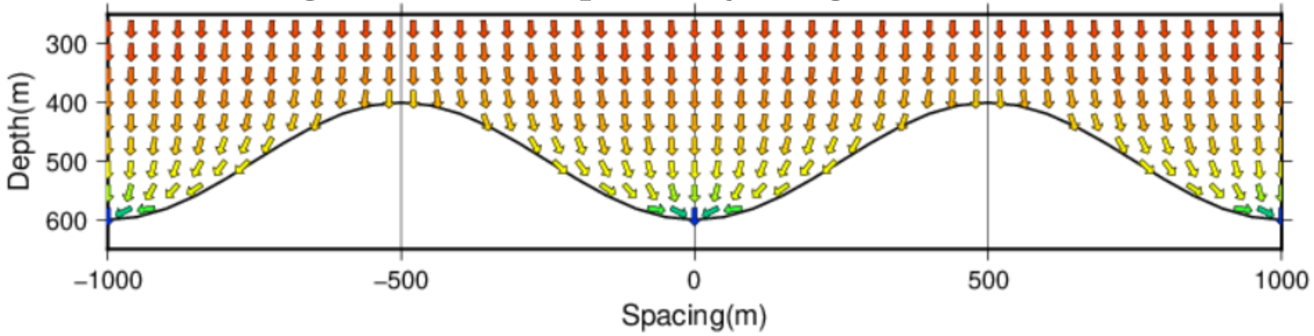

*The vectors have the same size, but their colors depend on the magnitudes.

- The TE-mode magnetic field becomes nearly vertical on submarine valleys.
- Anomalous behaviors of the TE-mode responses must be caused by the distorted magnetic field.
- I performed the Poynting vector analysis as Key & Constable (2011, *PEPI*) and Selway *et al.* (2012, *GJI*) did.
- The TE-mode Poynting vectors in the sea layer point toward submarine valleys.

Apparent resistivity & Phase   Tipper

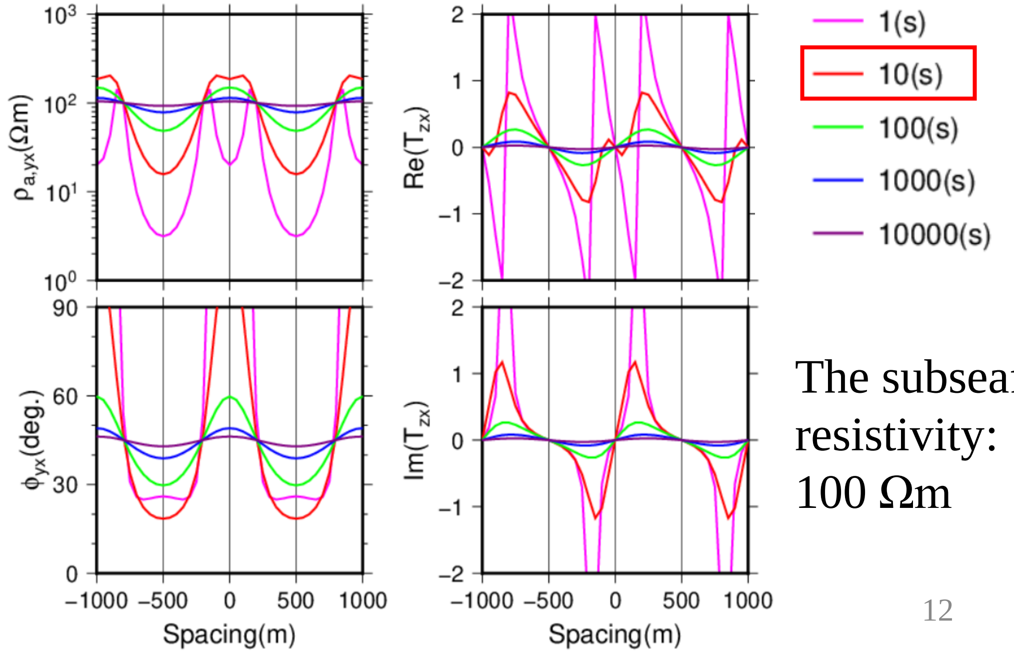

The subseafloor resistivity: 100 Ωm

Spatial distribution of MT response functions for a 2-D sinusoidal bathymetry (2)

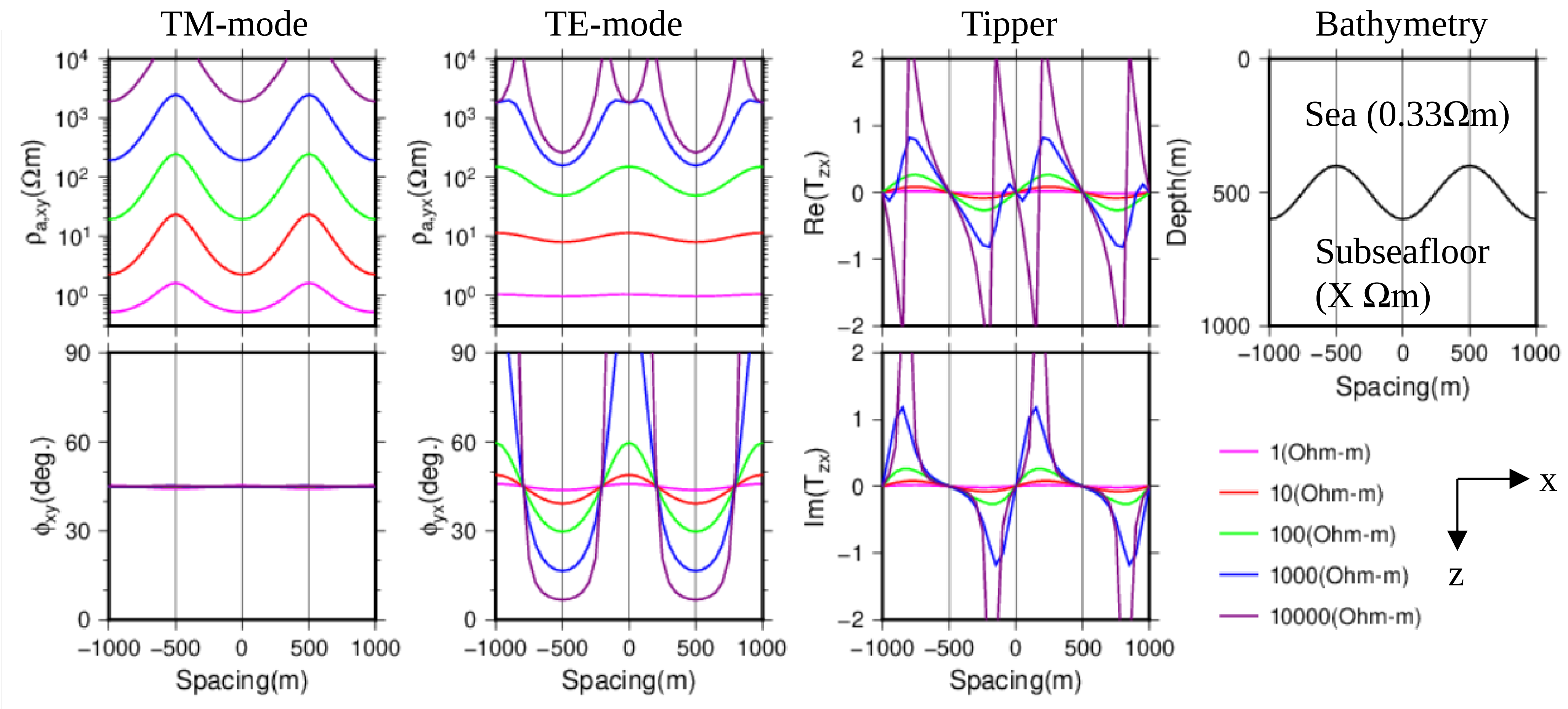

- MT response functions for different subseafloor resistivity with a fixed period (100 sec).
- Strength of bathymetry effects becomes large with increasing subseafloor resistivity.
- Bathymetry effects on the TM-mode apparent resistivity also depends on subseafloor resistivity.

Spatial distribution of MT response functions for a 2-D sinusoidal bathymetry (3)

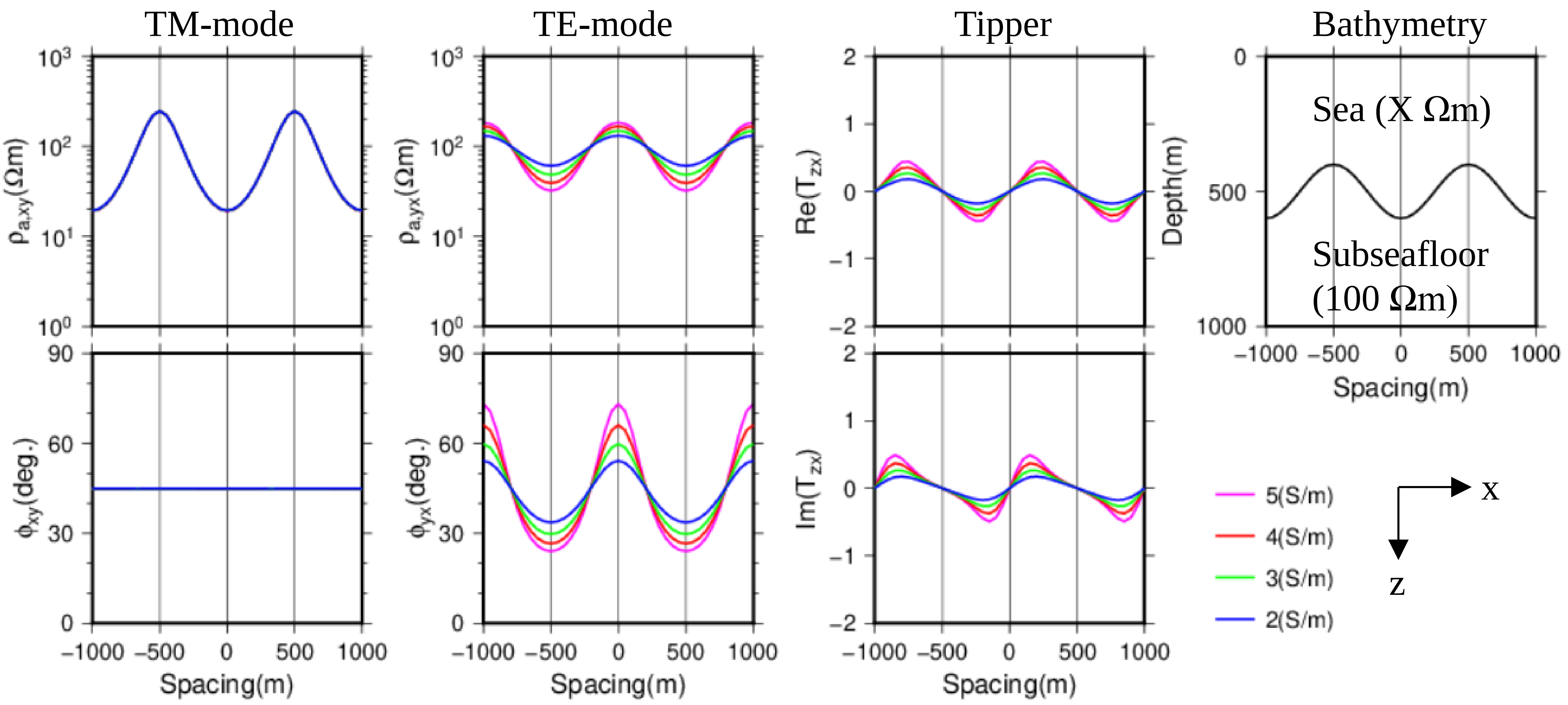

- MT response functions for different <u>resistivity of the sea</u> with a fixed period (100 sec).
- The TM-mode response functions are nearly independent of the sea resistivity.
- The TE-mode response functions depend on the sea resistivity.
- Bathymetry effects on the TE-mode responses become large with increasing conductivity of the sea.

Sounding curves for a 2-D sinusoidal bathymetry (1)

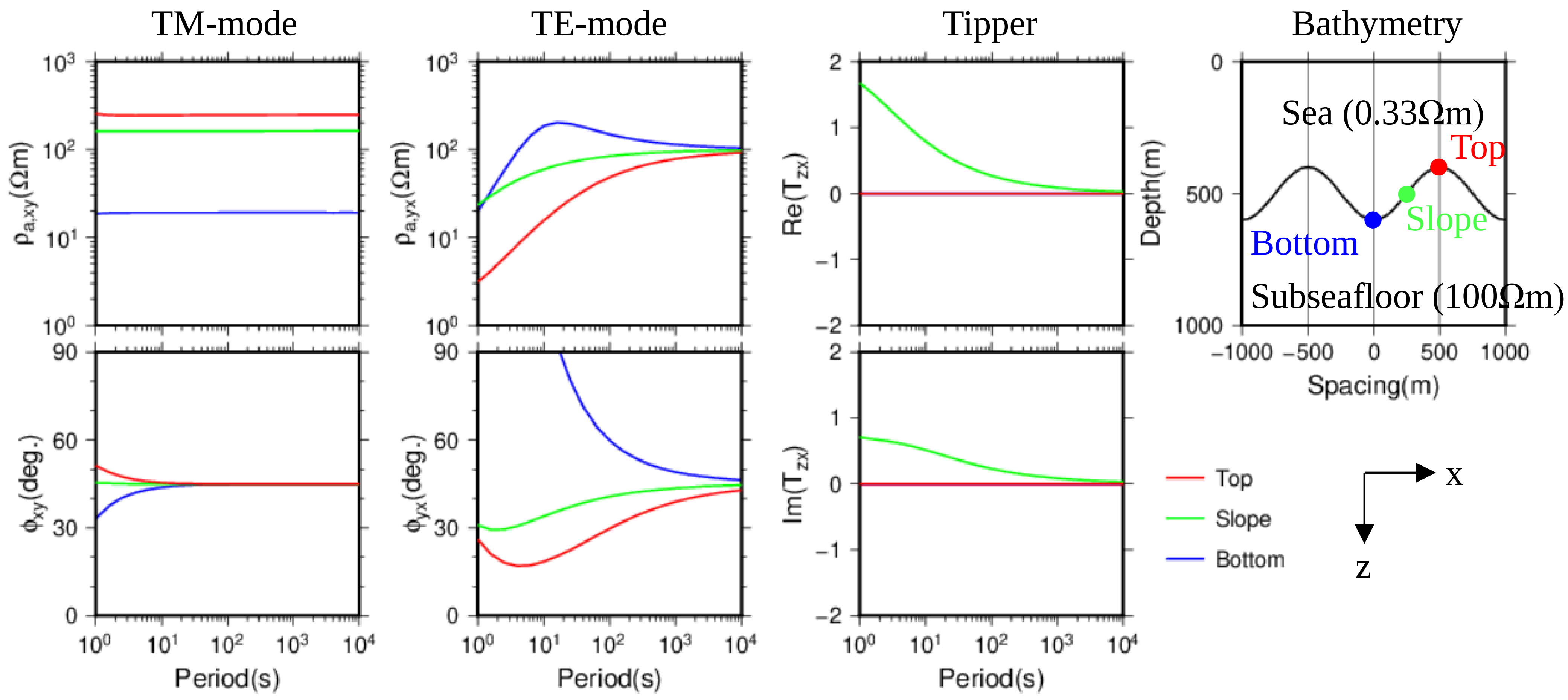

- Bathymetry effects become large with decreasing period similar to the land topography case.
- Bathymetry effects on the TM-mode response functions are comparable to land topography effects.
- Bathymetry effects on the TE-mode response functions are greater than land topography effects.

Sounding curves for a 2-D sinusoidal bathymetry (2)

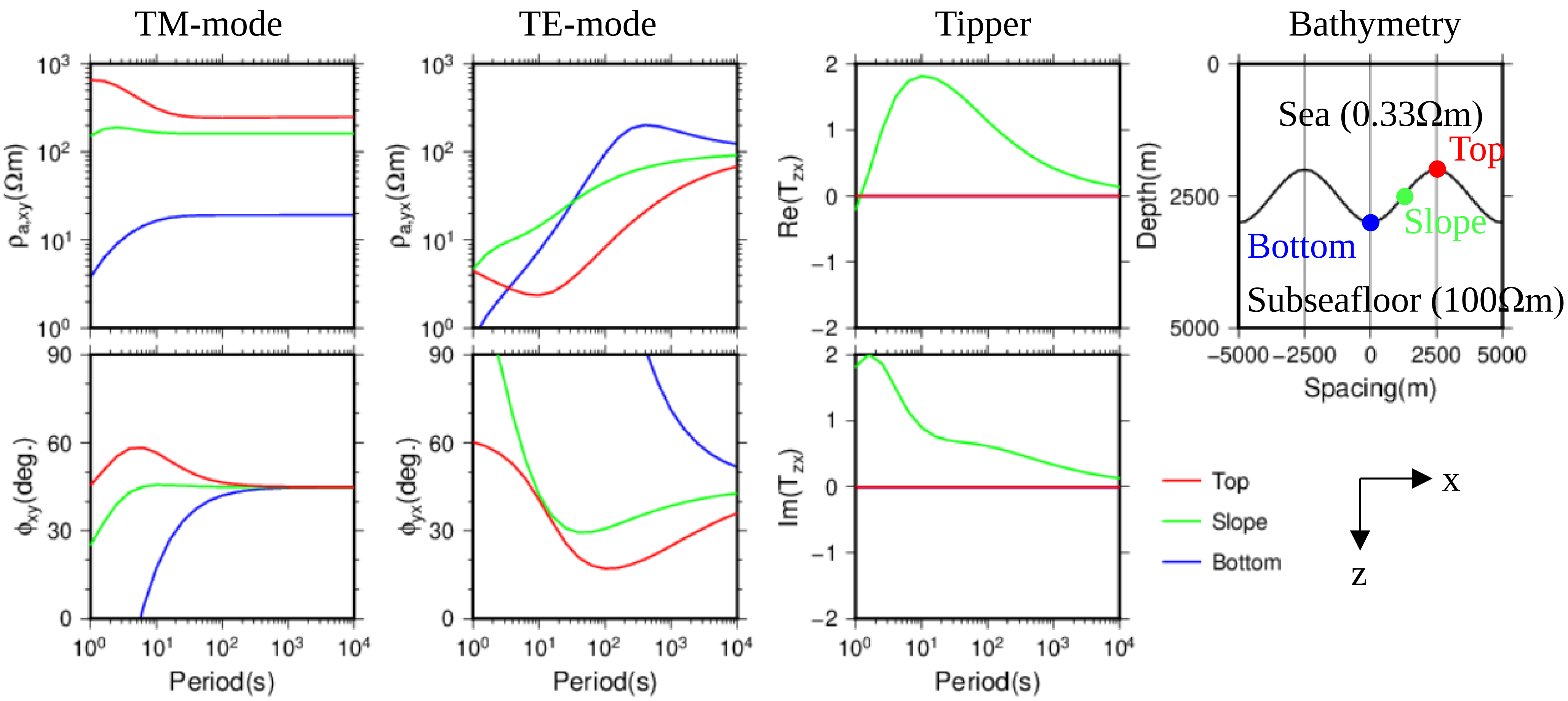

➢ Scale of undulation (amplitude and wavelength) is five times larger than the previous case.

➢ Bathymetry effects become large compared to the previous case.

➢ Bathymetry effects depend on the scale of the undulation.

Program used for calculating analytical MT response functions for a 2-D sinusoidal topography/bathymetry

The program for calculating analytical MT response functions for a 2-D sinusoidal undulation is available from GitHub.

https://github.com/yoshiya-usui/sinusoidal2DAna

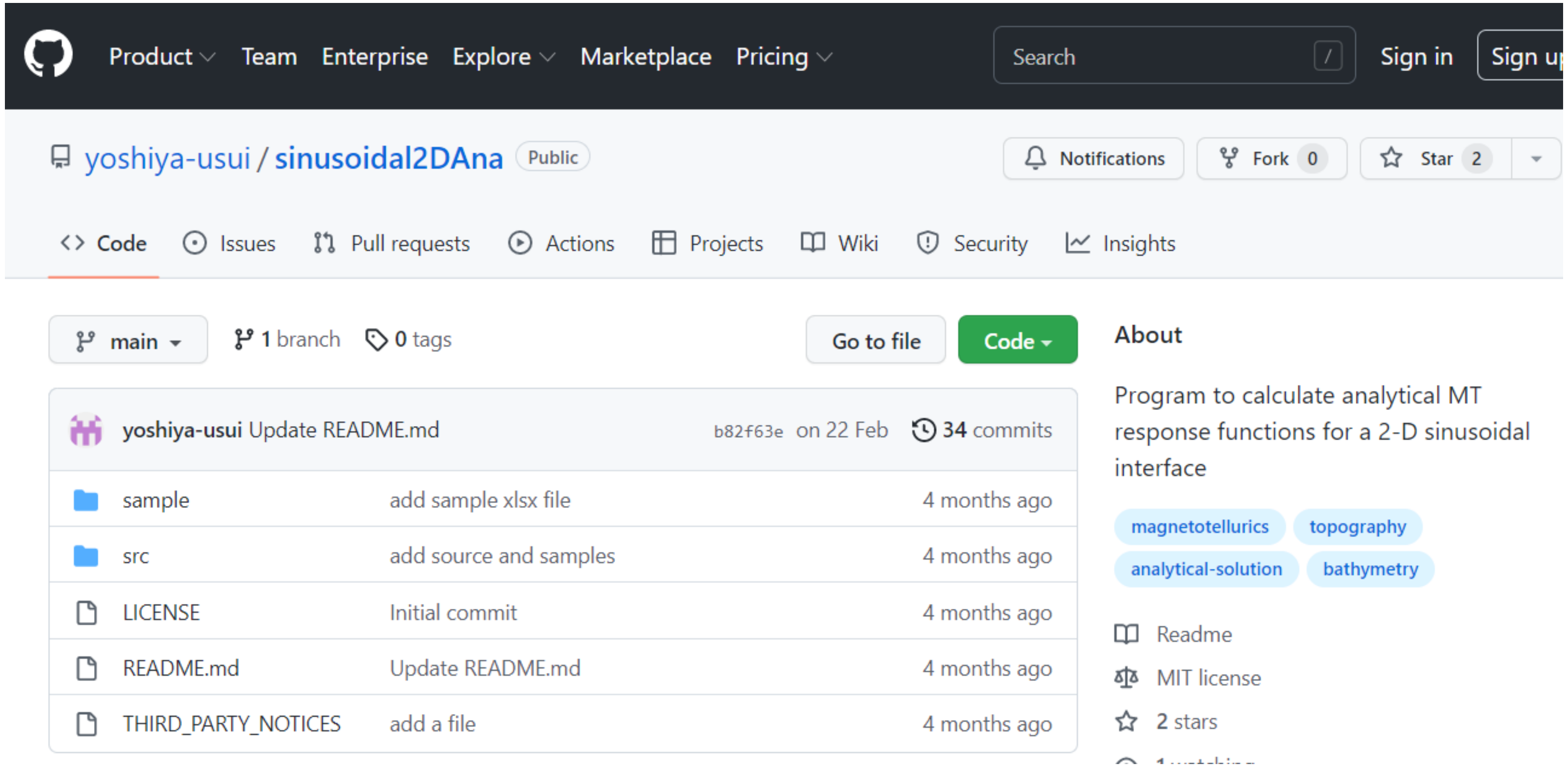

Topography effects of a 3-D trapezoidal hill

Nam *et al*. (2007, *Geophys. Prospect.*)

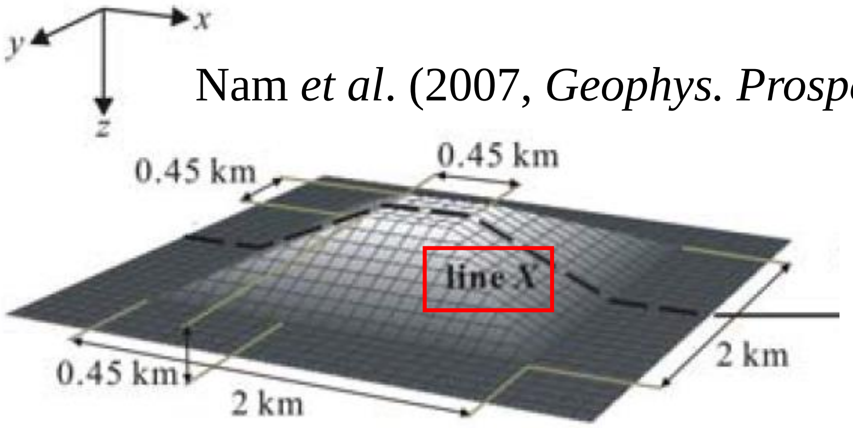

Subsurface (100 Ωm)

- Apparent resistivity is relatively small on the top of the hill.
- Apparent resistivity is relatively large on the foot of the hill.
- Phase increase on the top of the hill.
- Those features are consistent with 2-D topography effects.

Apparent resistivity @ 2 Hz

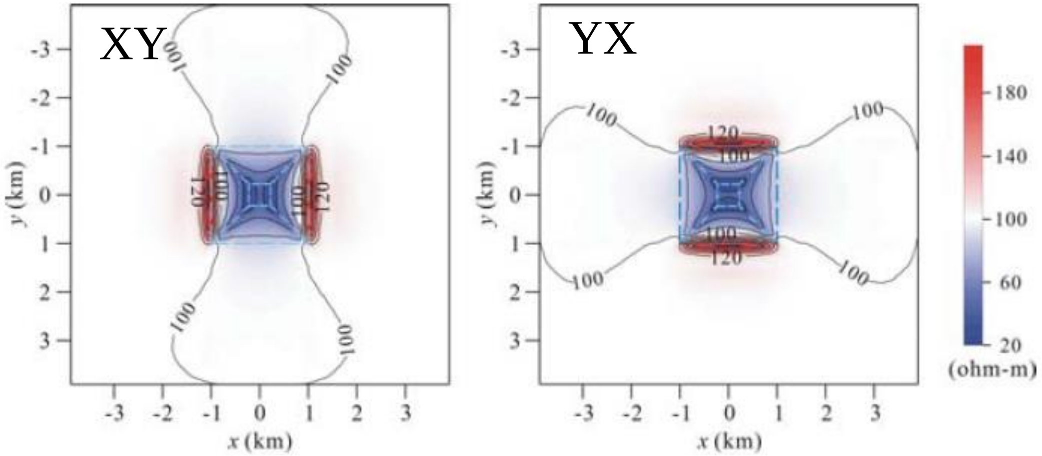

Apparent resistivity & phase @ 2 Hz on along line X (y = 0)

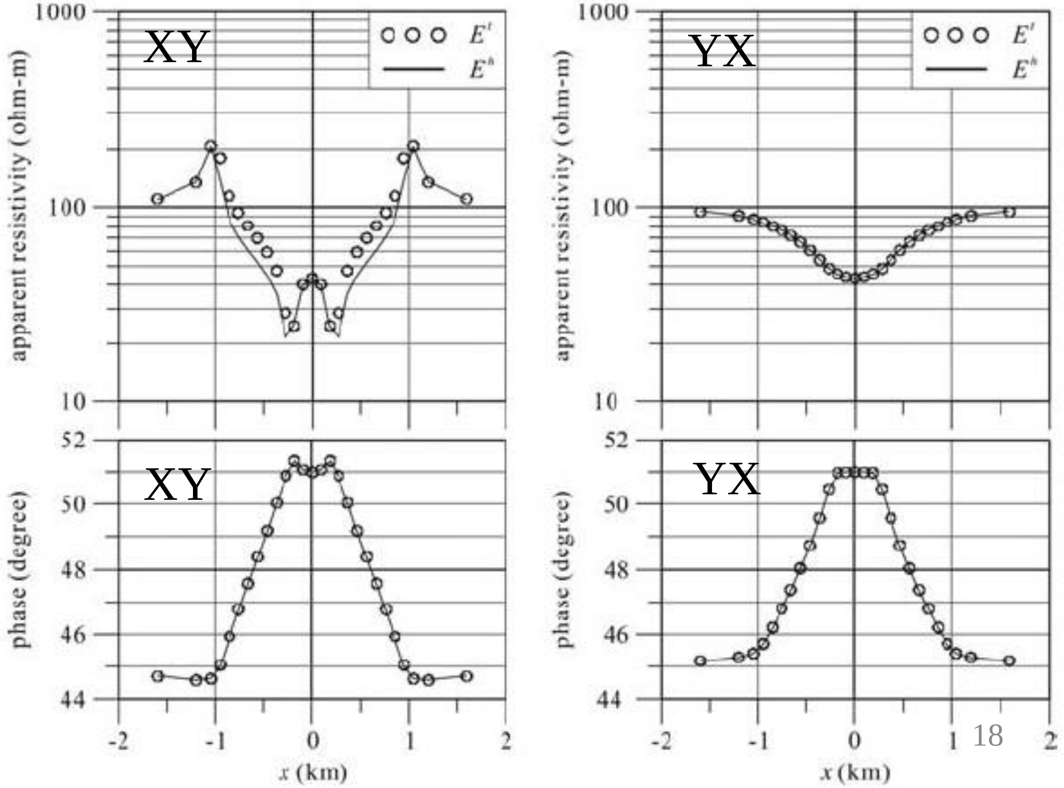

Topographic effects of real topography

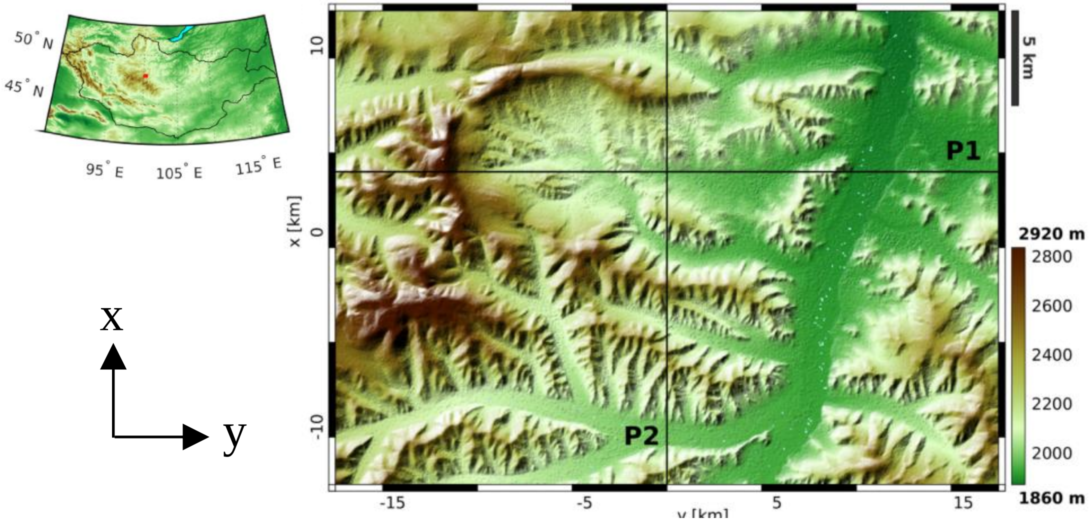

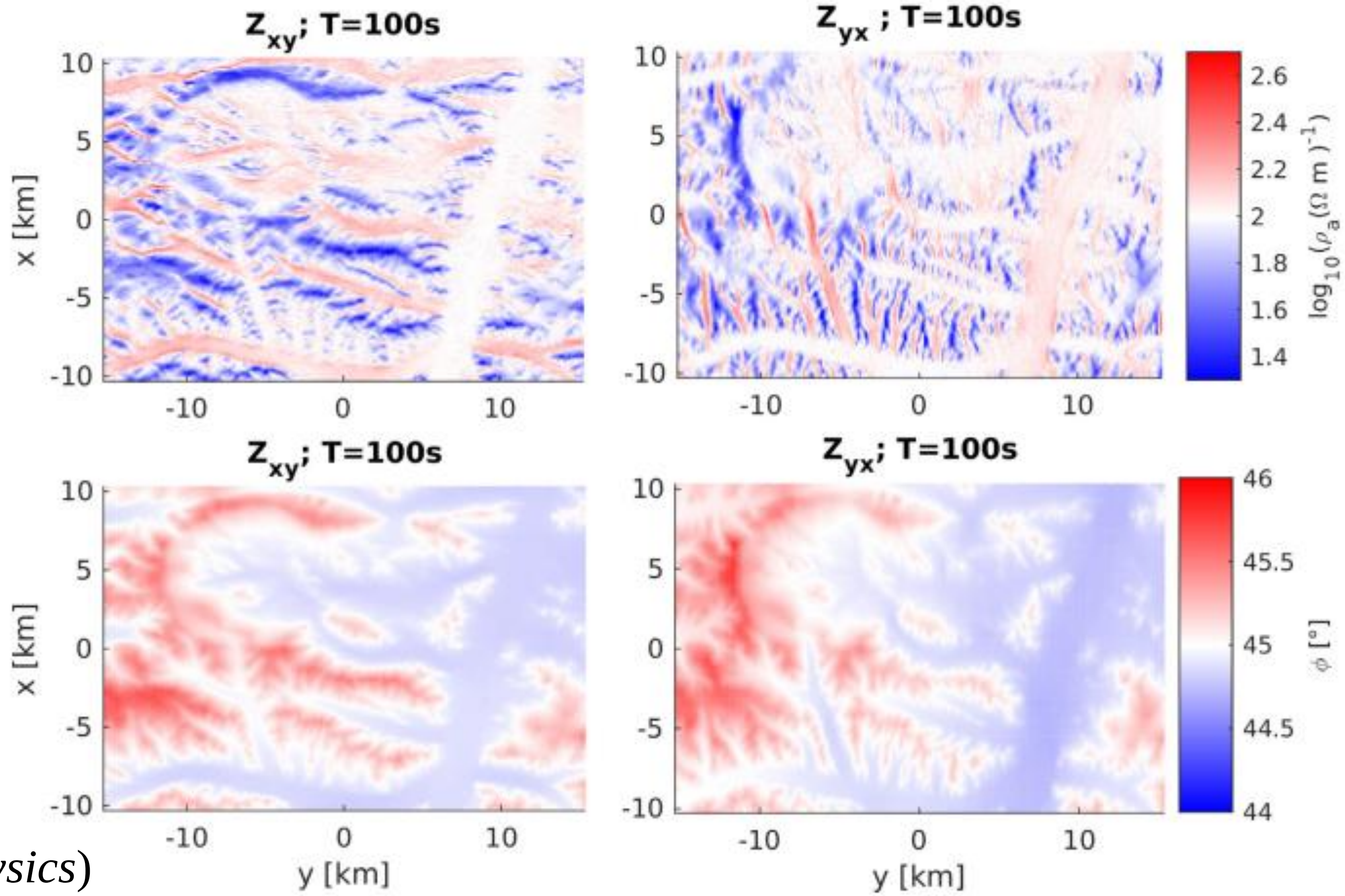

Käufl *et al.* (2018, *GJI*)

- Käufl *et al.* (2018, *GJI*) evaluated distortions due to real 3-D topography of the Hangai Mountains in Mongolia.
- They used GoFEM (Grayver & Kolev 2015, *Geophysics*) to compute the electromagnetic field.
- On hills, apparent resistivity decreases and phase increases.
- On valleys, apparent resistivity increases and phase decreases
- Induction arrows (Wiese convention) point away from tops of hills.
- Those results are also consistent with the 2-D topography effects.

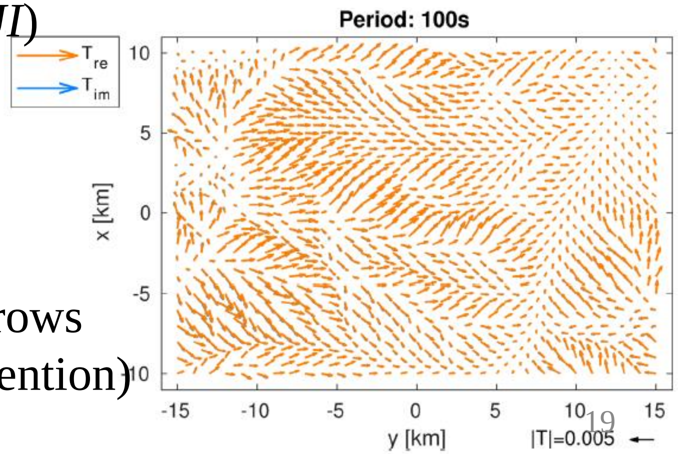

Induction arrows (Wiese convention)

Bathymetric effects of a Gaussian sea hill

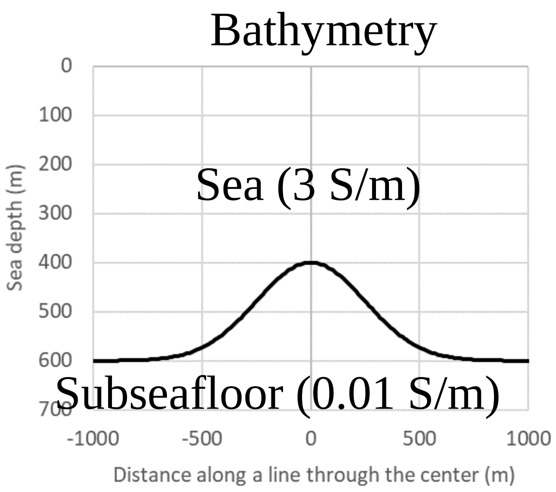

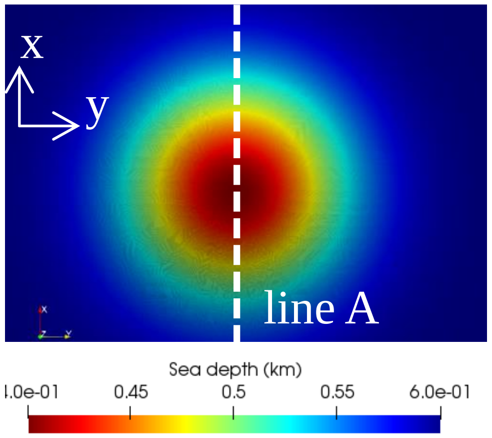

Spatial distribution of response functions along line A

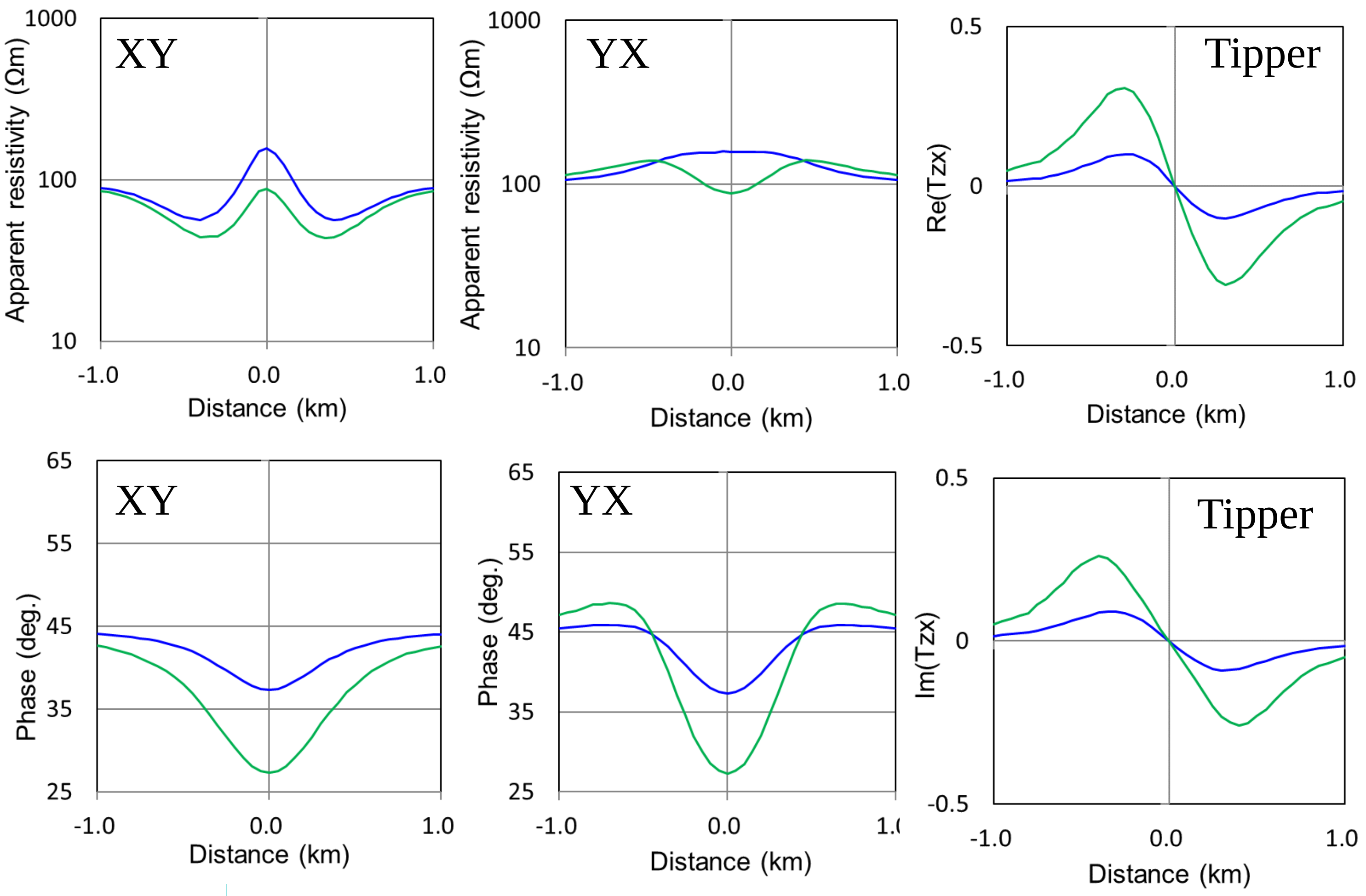

- I evaluated the bathymetry distortion due to a Gaussian sea mount.
- I used FEMTIC (Usui 2015; Usui *et al*. 2017, 2018, *GJI*) to compute the response functions.
- On the top of the sea mount, apparent resistivity increases and phase decreases.
- Bathymetry effects of the 3-D hill are more complex than the 2-D effects of a sinusoidal undulation.
- Combined effects of the TM-mode and TE-mode bathymetry effects appear in the response functions.

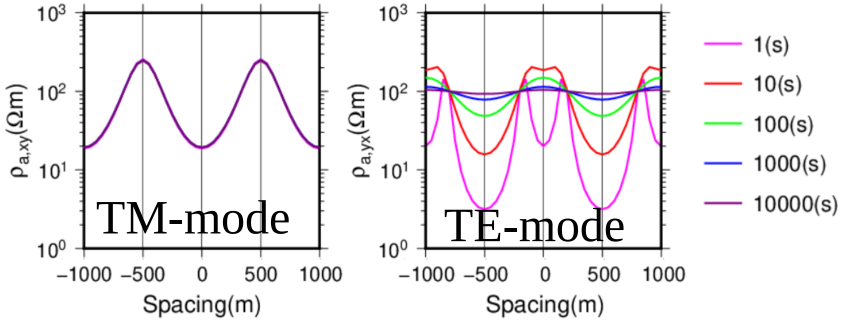

Coast effects on MT response functions

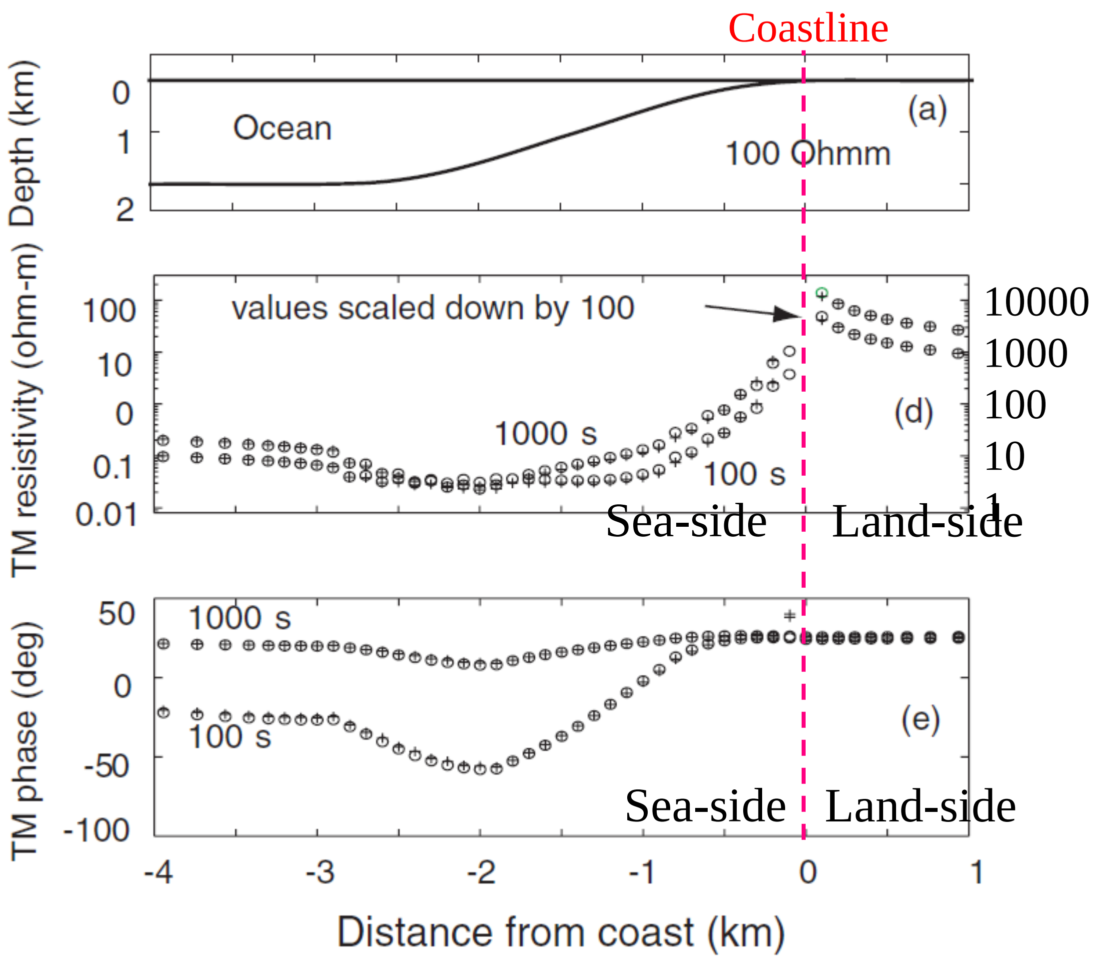

Li *et al*. (2008, *Geophys. Prospect.*)

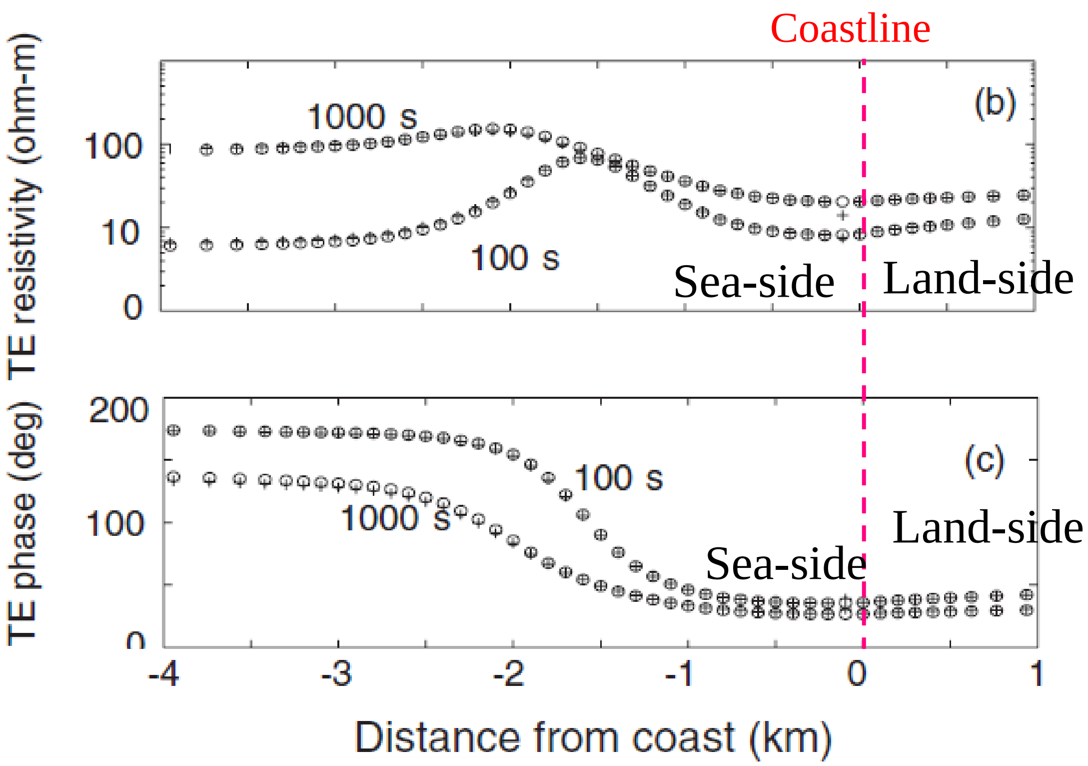

- Strong electrical conductivity contrast between the sea and the land can cause anomalous electromagnetic field near the coast.
- The land-side coast effect makes larger the TM-mode apparent resistivity of land MT stations.
- The ocean-side coast effect makes smaller the TM-mode apparent resistivity of ocean-bottom MT stations.
- Inductive distortion appears in the TE-mode response functions of ocean-bottom MT stations.

Coast effects on the TE-mode response functions (1)

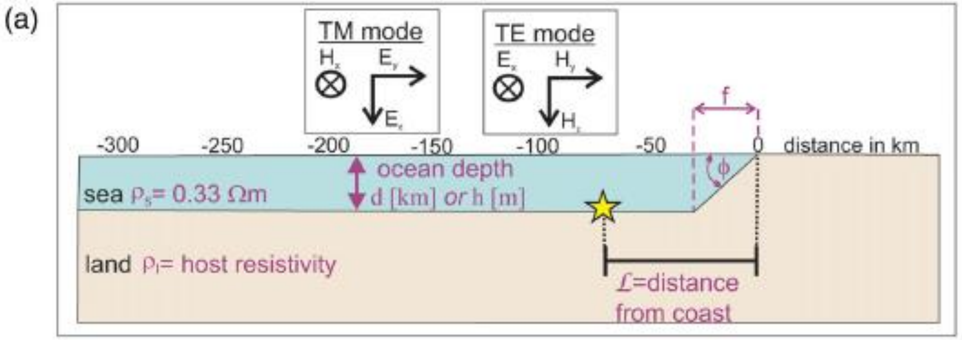

Worzewski *et al*. (2012, *GJI*)

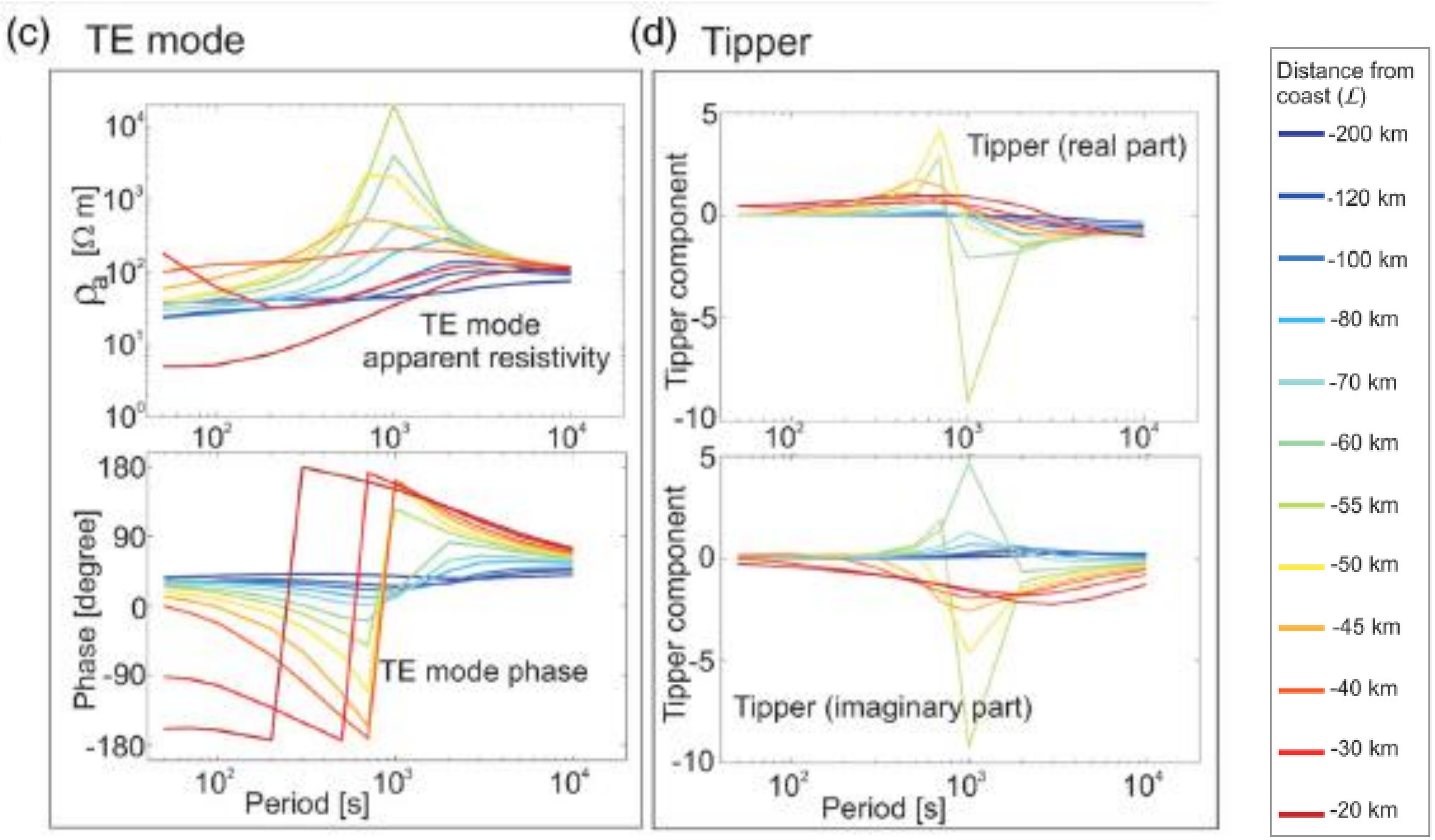

- ➢ The ocean-side coast effects on the TE-mode response functions have been studied recently (Constable *et al*. 2009, *GJI*; Key & Constable 2011, *PEPI*; Worzewski *et al*. 2012, *GJI*).
- ➢ The ocean-side coast effect can produce cusps in apparent resistivity and out-of-quadrant phases in the TE-mode.
- ➢ Even such a simple 2-D bathymetry can cause cusps, anomalous phases, and anomalously large tipper.

Coast effects on the TE-mode response functions (1)

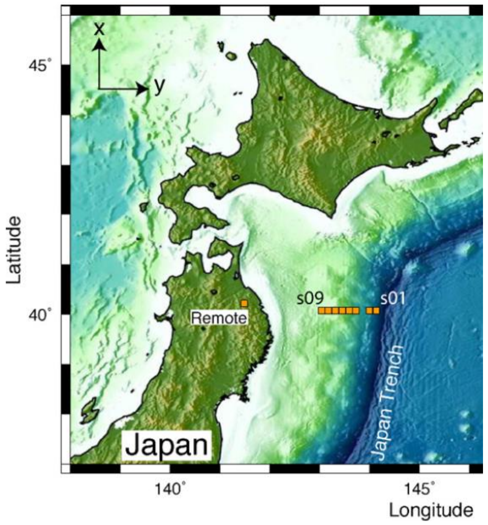

2D model of the Japan island trench and deep-ocean plain

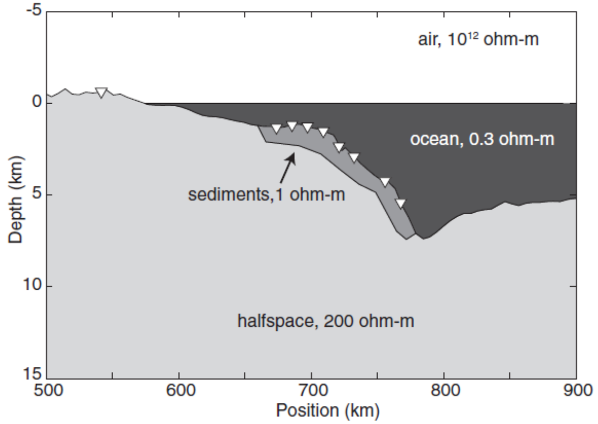

Key & Constable (2011, *PEPI*)

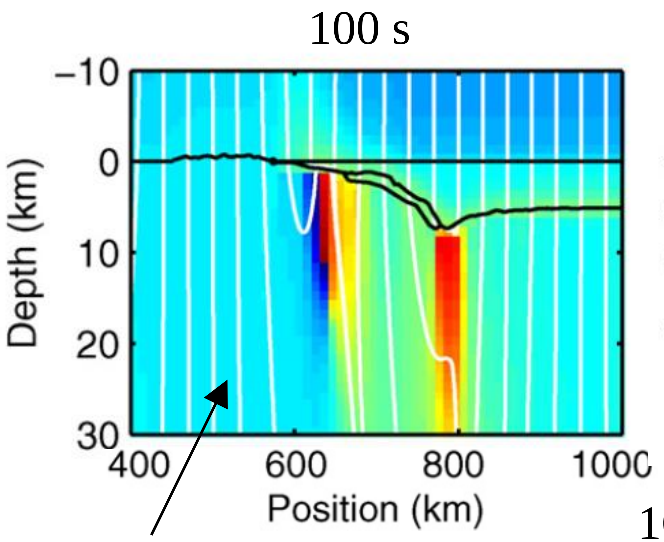

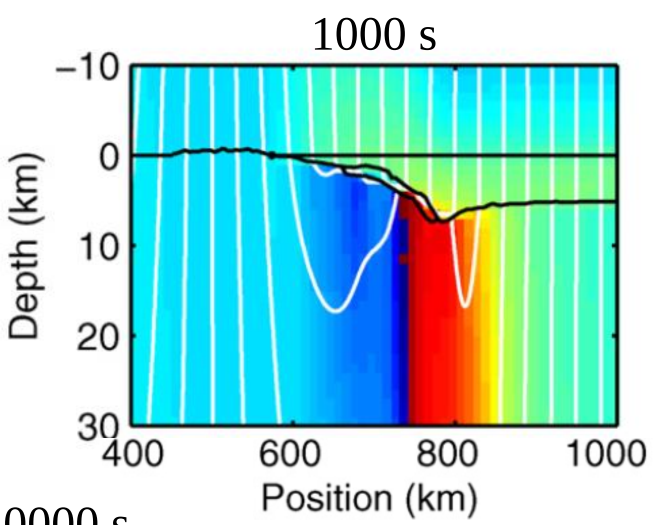

Streamlines of the time-averaged complex Poynting vector

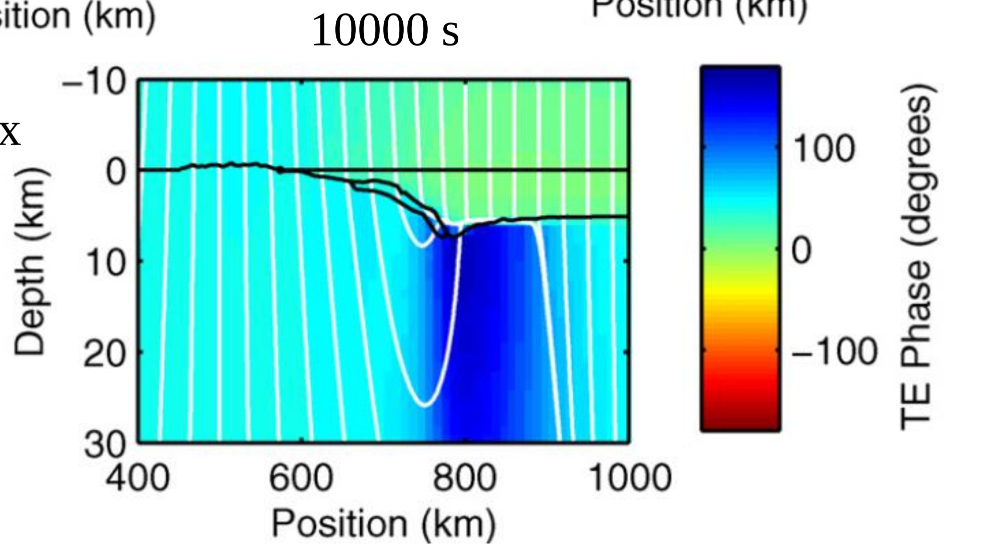

- Key & Constable (2011, *PEPI*) investigated the cause of the strong coast effects on the TE-mode response functions.
- They showed that the anomalous TE-mode response functions are caused by the distorted magnetic field. They found the magnetic field has a minimum amplitude around a characteristic frequency.
- Their Poynting vector analysis showed that out-of-quadrant phases are associated with the upward energy flow to the seafloor.

Agenda

1. Influences of topography and bathymetry on MT response functions

2. Review of the methods to incorporate topography and bathymetry in 3-D MT modeling

3. Brief introduction of 3-D MT inversion code FEMTIC

Modeling of 3-D topography with a FDM code

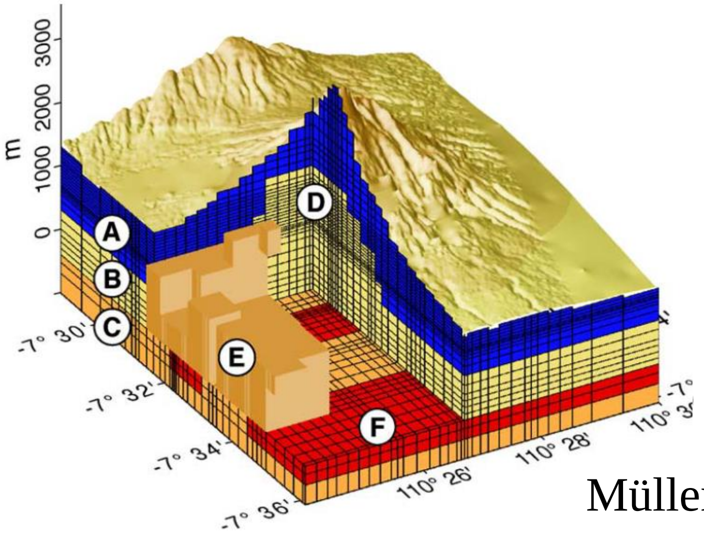

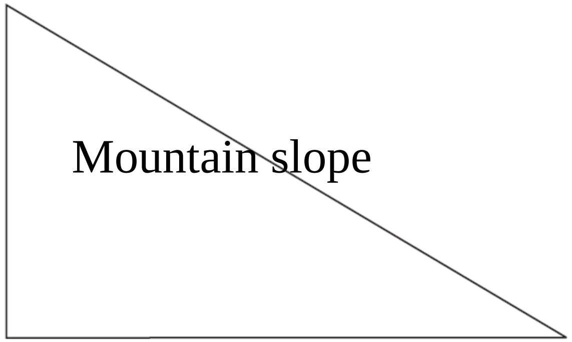

Müller & Haak (2004, *JVGR*)

Apparent resistivity curves appear unstable, displaying large jumps between narrow period bands

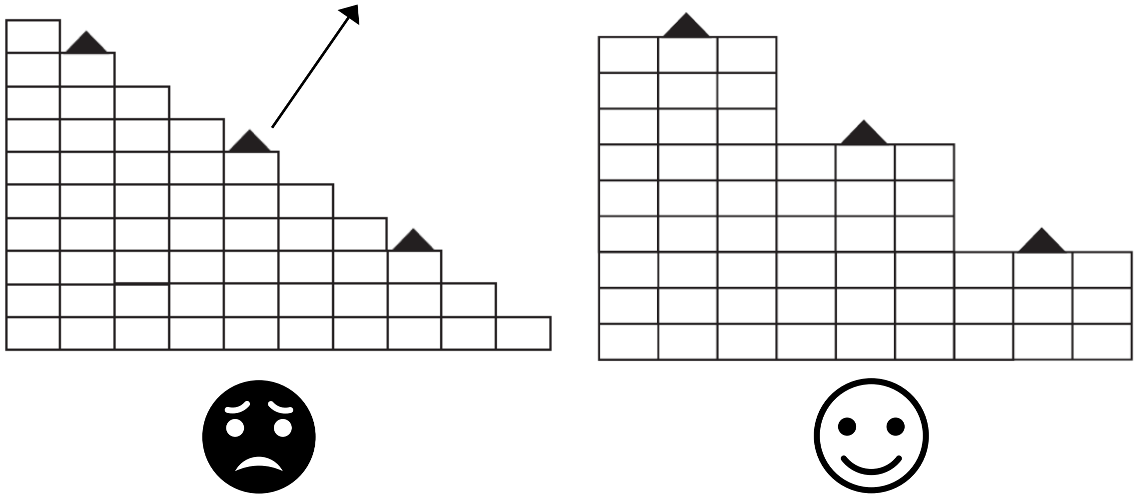

- ➢ The most common approach to include land topography is modeling a smooth dipping surface by a sequence of steps with rectangular cells.
- ➢ Müller & Haak (2004, *JVGR*) derived a 3-D resistivity structure of Merapi volcano in Central Java by such modeling.
- ➢ They reported that flat areas with two additional blocks in each direction from the observation points gave sufficient results.
- ➢ Whether additional blocks are required or not may depend on survey area and forward calculation scheme.
- ➢ Anyway, when we use rectangular cells, a fine horizontal grid would be necessary to accurately calculate the electromagnetic field on an undulating surface.

Modeling of 3-D bathymetry with a FDM code

Baba & Seama (2002, *GJI*)

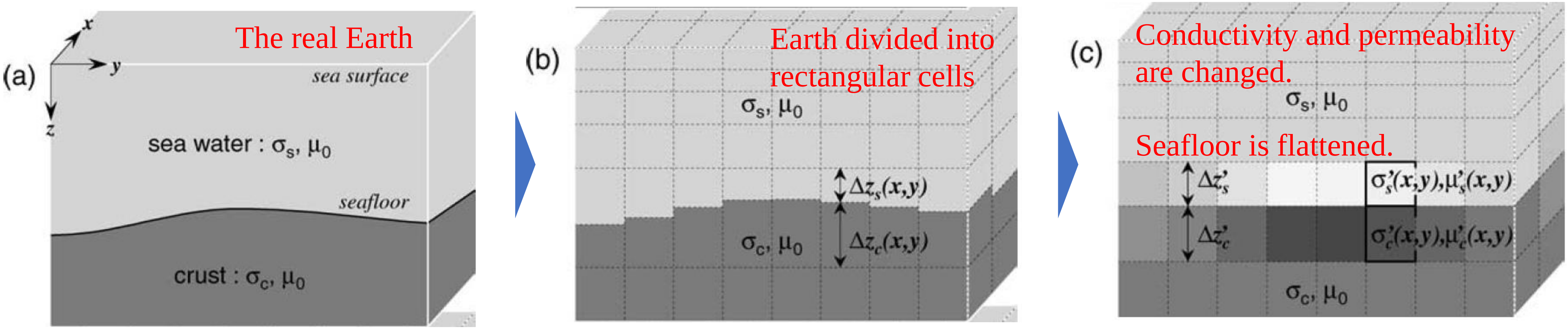

- Bathymetry effects on ocean-bottom MT data are much more severe than topography effects on land MT data.
- Baba & Seama (2002, *GJI*) proposed a modeling technique, called FS3D, to incorporate 3-D seafloor undulations in FDM forward calculation.
- FS3D converts seafloor undulations to spatial changes in the electrical conductivity and magnetic permeability of cells bounding a flat-lying seafloor (conductance and the permeance are conserved in the x, y, and z directions).
- Baba & Chave (2005, *JGR*) developed a mantle structure inversion algorithm using FS3D.

1. MT response functions with and without 3-D bathymetry are calculated by FS3D.
2. Bathymetry effect term $\boldsymbol{Z}_t$ is estimated. $\boldsymbol{Z} = \boldsymbol{Z}_t \boldsymbol{Z}_m$ ($\boldsymbol{Z}$: With bathymetry; $\boldsymbol{Z}_m$: Without bathymetry)
3. Bathymetry effect is removed from the observed impedance tensor $\boldsymbol{Z}_c = \boldsymbol{Z}_t^{-1} \boldsymbol{Z}_o$ ($\boldsymbol{Z}_c$: Corrected; $\boldsymbol{Z}_o$: Observed)
4. Subseafloor resistivities are updated using the corrected impedance tensors

(These procedures are repeated)

3-D marine FDM inversion including bathymetry

Tada *et al.* (2012, *EPS*)

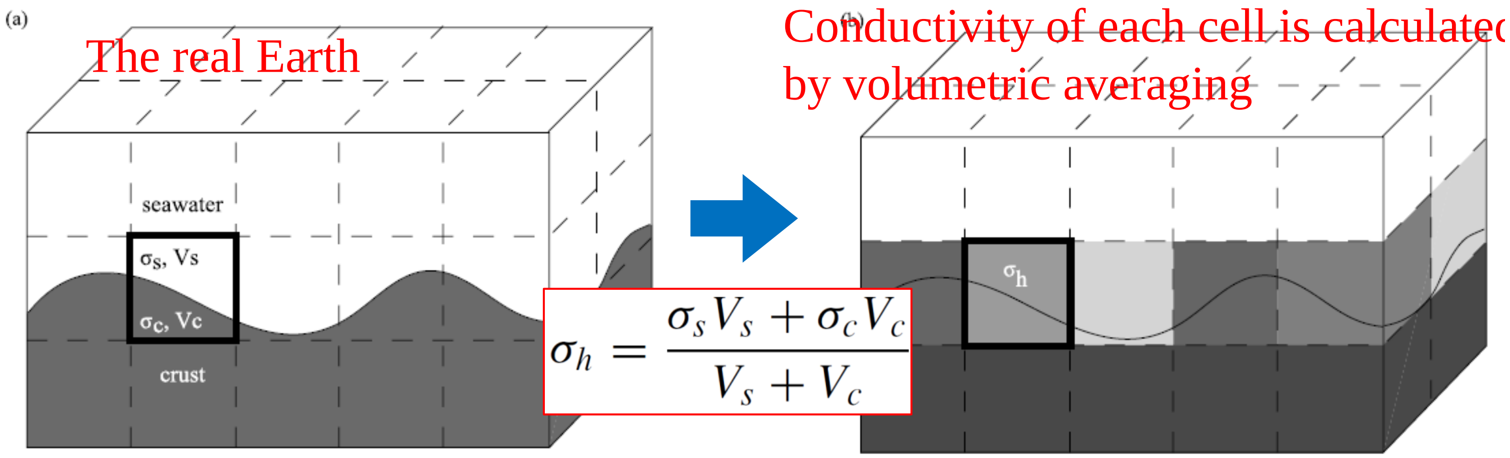

$$\sigma_h = \frac{\sigma_s V_s + \sigma_c V_c}{V_s + V_c}$$

FDM grid and magnetic field components

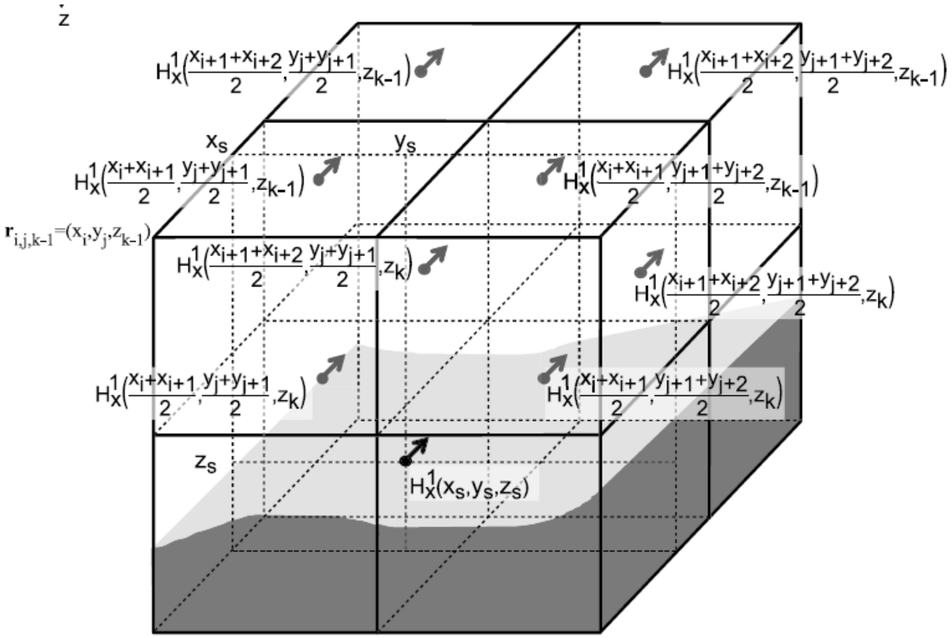

- ➢ Tada *et al.* (2012, *EPS*) proposed an approximate treatment of 3-D bathymetry to reveal regional-scale mantle structures.
- ➢ Tada *et al.* (2012, *EPS*) modified a 3-D FDM code, WSINV3DMT (Siripunvaraporn *et al*. 2005, *PEPI*), to incorporate bathymetry into a numerical grid.

  1. Conductivity of each seafloor cell is calculated by volumetric averaging of the sea resistivity and subseafloor resistivity
  2. The electromagnetic field on each ocean-bottom MT station is calculated by spatial interpolation and extrapolation.

- ➢ Sensitivity matrix (Jacobian) is also modified to conform to the above treatments.

Two-stage modelling scheme based on FDM codes

First stage

Calculate $\boldsymbol{Z}^{rs}$ using the grid that contains only large-scale structure based on the method of Tada *et al.* (2012)

↓

Second stage

Calculate $\boldsymbol{Z}^{ts}$ using the grids that contains small-scale topography based on FS3D (Baba & Seama 2002)

↓

Calculate local topographic distortion term $\boldsymbol{D}^{lt}$ for each site and frequency.

↓

Update subseafloor resistivities based on the grid used in the first stage using distortion terms $\boldsymbol{D}^{lt}$.

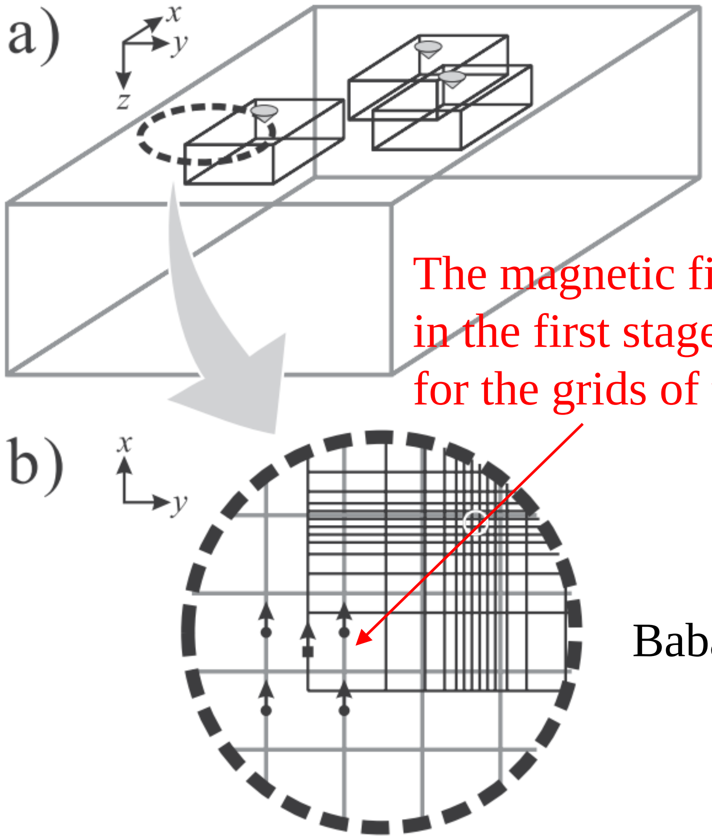

The magnetic field values output in the first stage are interpolated for the grids of the second stage.

Baba *et al.* (2013, *GJI*)

- Baba *et al.* (2013, *GJI*) proposed a two-stage modelling scheme that can simulate the effects of local small-scale bathymetry and regional large-scale bathymetry.
- This two-stage scheme is practical and has been used to reveal mantle structures beneath the Pacific Ocean and the Atlantic Ocean (Tada *et al.* 2014, *G^3*; Baba *et al.* 2016, *Tectonophysics*).

Correction equation

$$\boldsymbol{Z}^{ts}(\boldsymbol{r},\omega) \approx \boldsymbol{D}^{lt}(\boldsymbol{r},\omega)\, \boldsymbol{Z}^{rs}(\boldsymbol{r},\omega)$$

Local topographic distortion term

Response to the structure only with large-scale topography

Modeling of 3-D topography using a FEM code

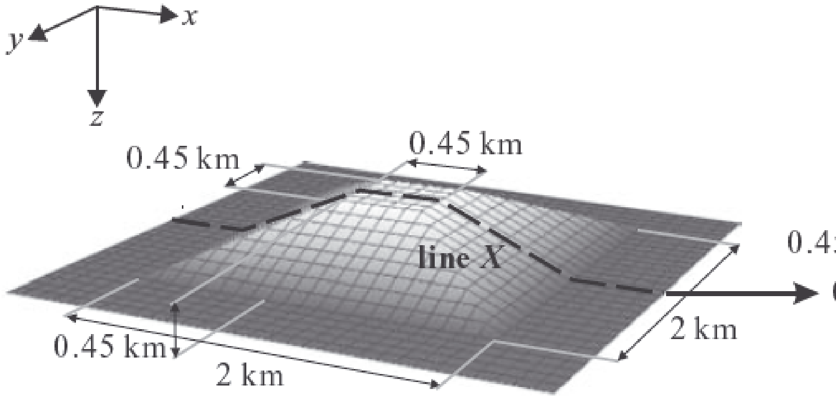

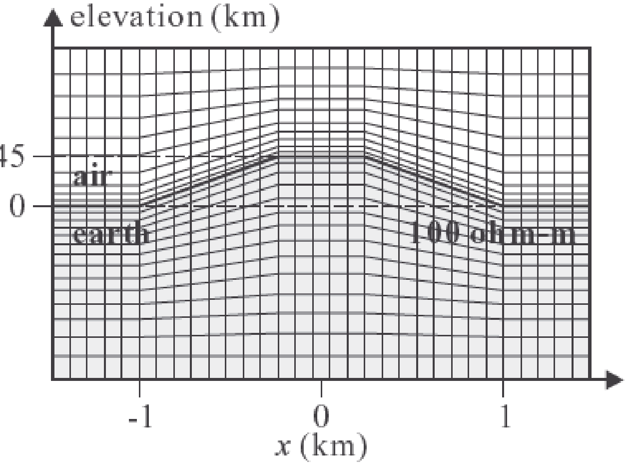

Nam *et al.* (2008, *GJI*)

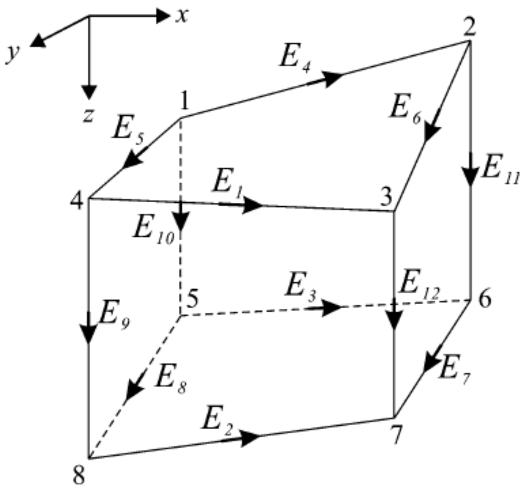

Nam *et al.* (2007, *Geophys. Prospect.*)

- Recently, the finite element method (FEM) has been used in MT forward modeling and inversion.
- Because deformed elements can be used in the FEM, we can accurately incorporate topography and bathymetry into a computational mesh.
- Several types of elements can be used in the FEM.
- Nam *et al.* (2007, *Geophys. Prospect.*) developed an MT forward modeling code using deformed hexahedral elements.
- Nam *et al.* (2008, *GJI*) developed an MT inversion method using the FEM code of Nam et al. (2007, *Geophys. Prospect.*).
- Nam *et al*. (2008, GJI) used the FEM only for evaluating topography effects term. Inversion itself was performed by a FDM code (Sasaki *2001*, *J. Appl. Geophys.*) after topography effect correction similar to Baba & Chave (2005, *JGR*).

3-D MT inversion using the deformed hexahedral element

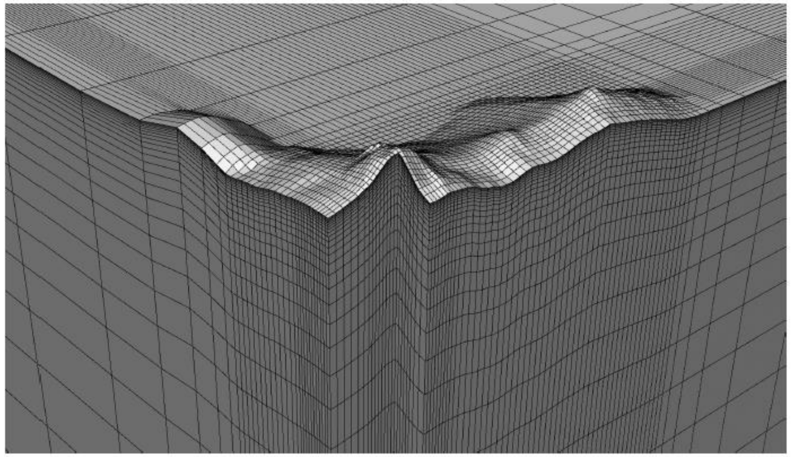

Kordy *et al.* (2016, *GJI*)

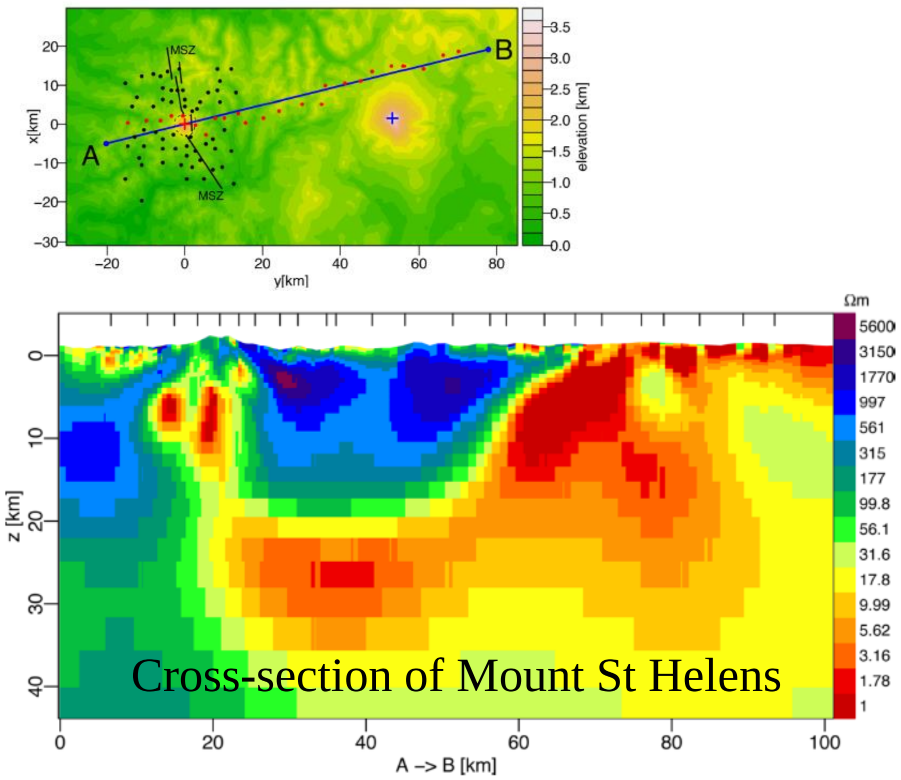

Cross-section of Mount St Helens

Kordy *et al.* (2016, *GJI*)

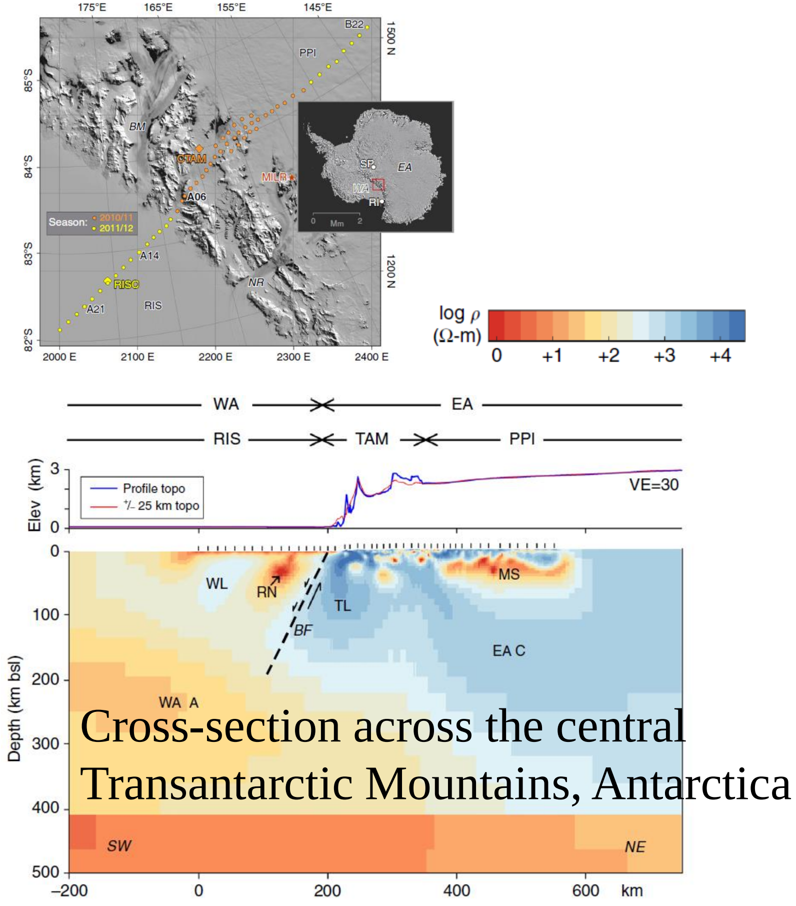

Cross-section across the central Transantarctic Mountains, Antarctica

Wannamaker *et al.* (2017, *Nat. Commun.*)

- Kordy *et al.* (2016, *GJI*) (consisting of two papers) developed a 3-D MT inversion method using the deformed hexahedral element.
- A data-space Gauss-Newton algorism was used to speed up the inversion.
- The inversion code of Kordy *et al.* (2016, *GJI*) has been applied to several MT data measured on steep mountains.

For example, Mount St Helens (Kordy et al. 2016, GJI) and Transantarctic Mountains, Antarctica (Wannamaker et al. 2017, Nat. Commun.)

3-D MT inversion using non-conforming hexahedral mesh

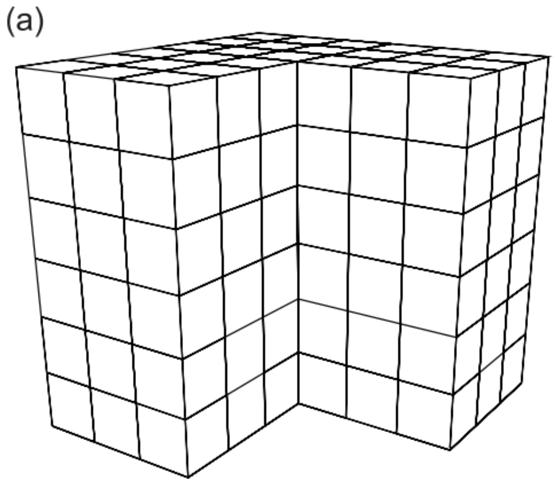

Grayver & Bürg (2014, *GJI*)

Mesh of the Kronotsky volcano model

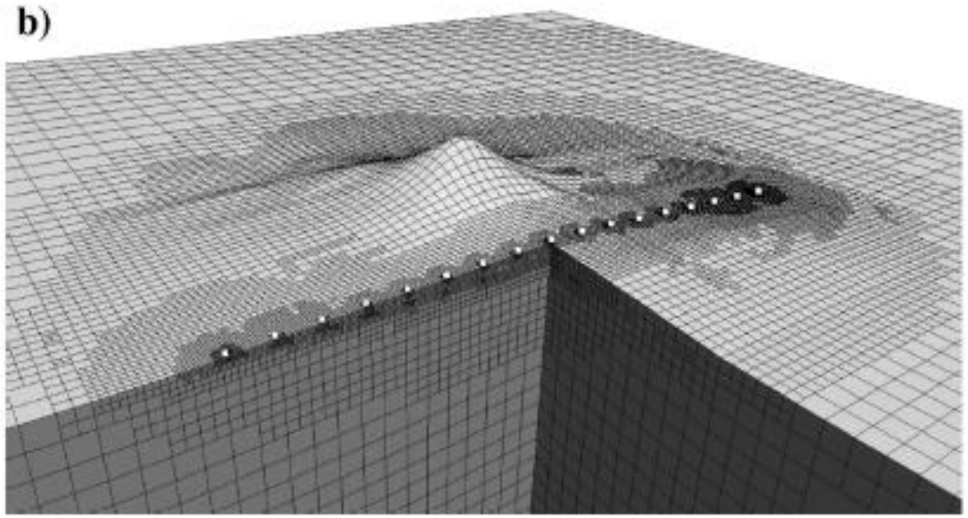

Grayver & Kolev (2015, *Geophysics*)

- Grayver & Bürg (2014, *GJI*) developed a 3-D MT inversion method using non-conforming hexahedral mesh.
- Grayver & Kolev (2015, *Geophysics*) developed a 3-D MT inversion method using higher-order elements.
- Term "non-conforming" means that one or more irregular hanging nodes exist on some element edges.
- Non-conforming element enables us to locally refine mesh only around observation stations, that saves computational costs.
- The degree of freedoms (DOFs) of the fine side are related to DOFs of the coarse side by equations for constraints.

Hanging node

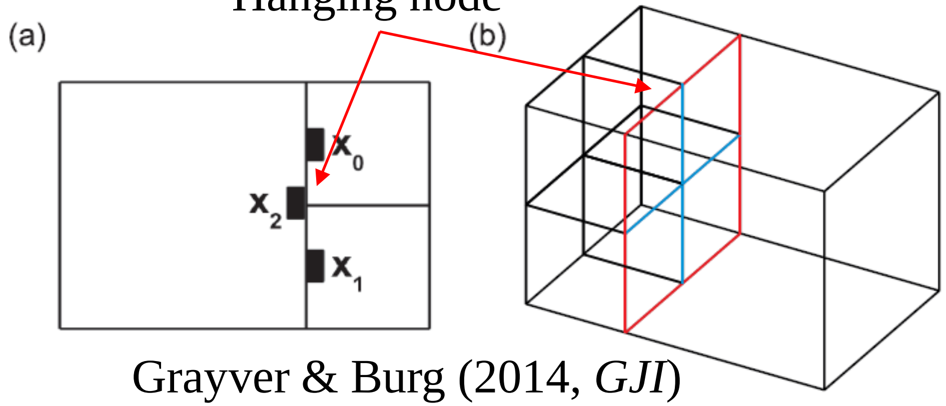

Grayver & Burg (2014, *GJI*)

$$x_0 = \frac{x_2}{2} \qquad x_1 = \frac{x_2}{2}$$

Applications of MT inversion using non-conforming hexahedral meshes

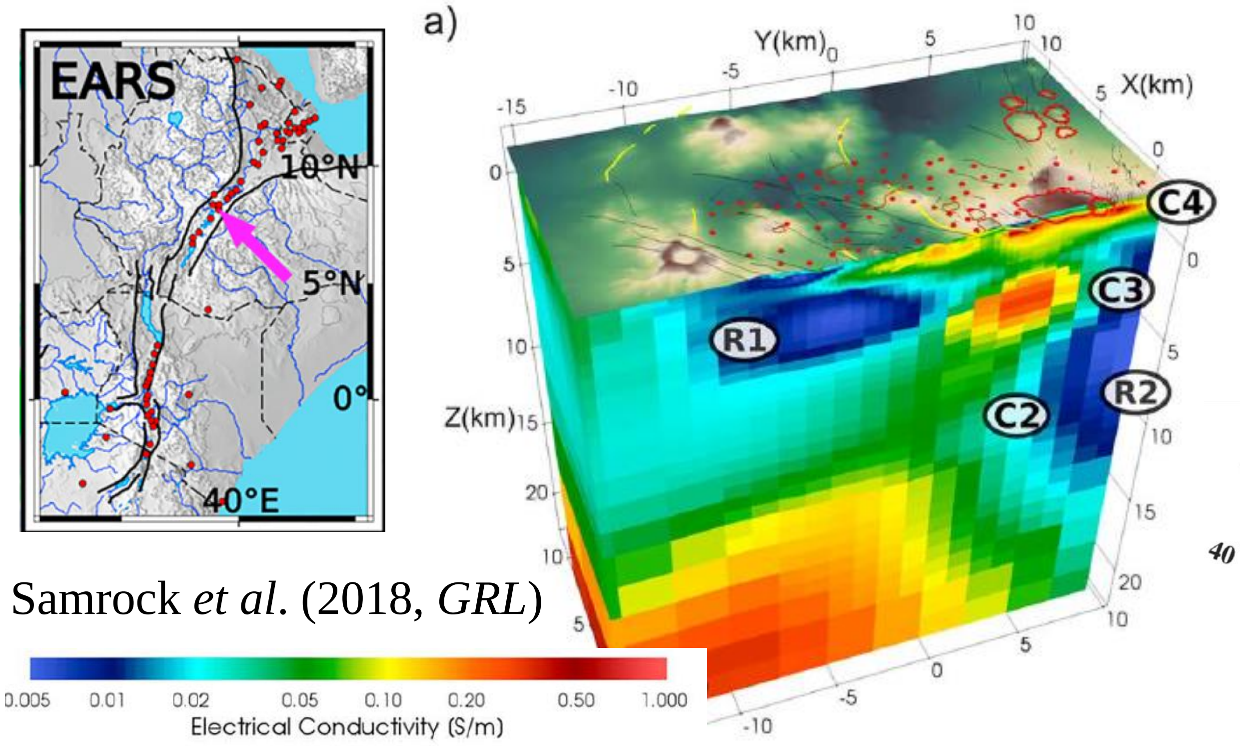

Samrock *et al*. (2018, *GRL*)

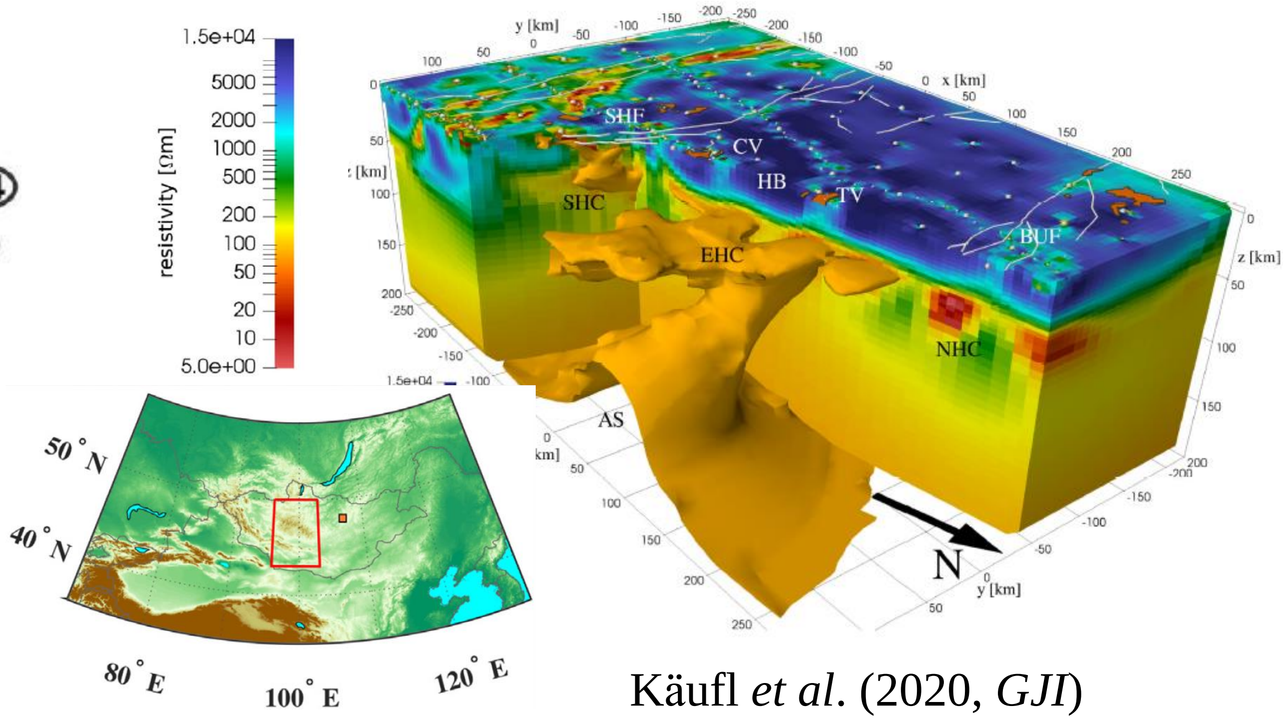

Käufl *et al*. (2020, *GJI*)

- Inversion code of Grayver & Kolev (2015, *Geophysics*), GoFEM, is very practical and has been applied to several MT data measured on tectonically active areas.
- Samrock *et al*. (2018, *GRL*) revealed a crustal-scale electrical conductivity model for a magmatic segment in the Ethiopian Rift.
- Käufl *et al*. (2020, *GJI*) revealed a 3-D crustal and upper mantle structure in the Hangai and Gobi-Altai region, central Mongolia.

3-D MT forward calculation using tetrahedral mesh

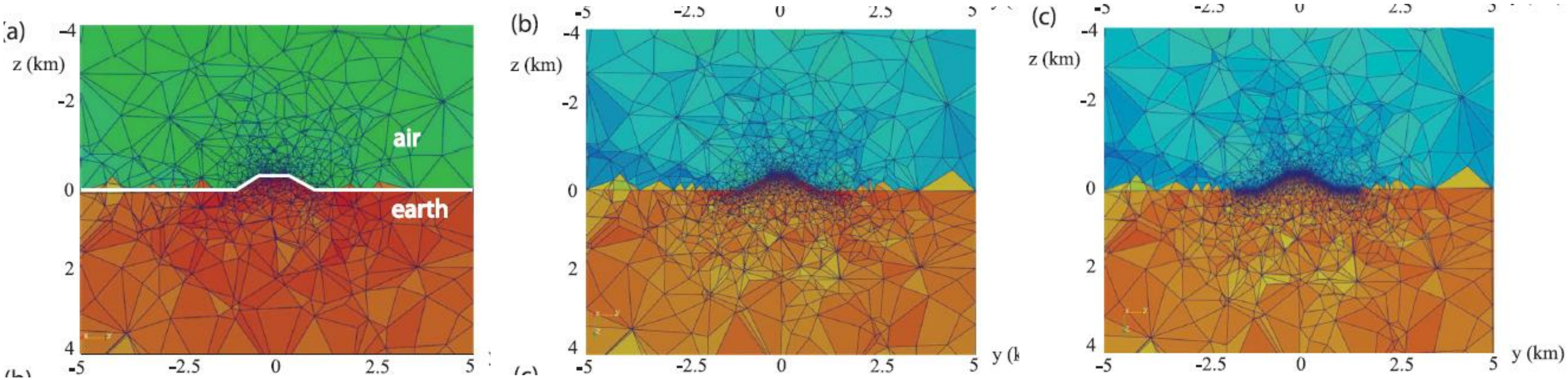

Ren *et al*. (2013, *GJI*)

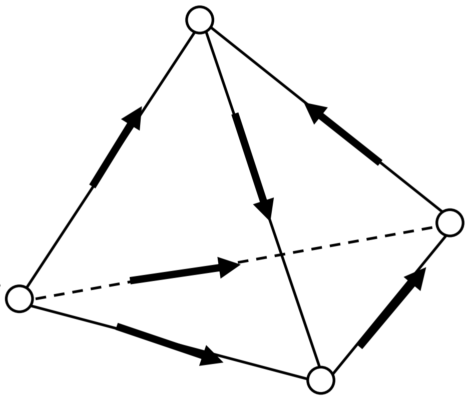

- Another well-used element in the 3-D FEM is the tetrahedral element.
- Tetrahedral element also enables us to locally refine mesh only around observation stations, that saves computational costs.
- Ren *et al.* (2013, *GJI*) developed a 3-D MT forward calculation method using tetrahedral element.
- The method of Ren *et al.* (2013, *GJI*) seeks an optimal mesh density distribution by an adaptive mesh refinement technique to ensure accurate solutions.

3-D MT inversion using tetrahedral mesh

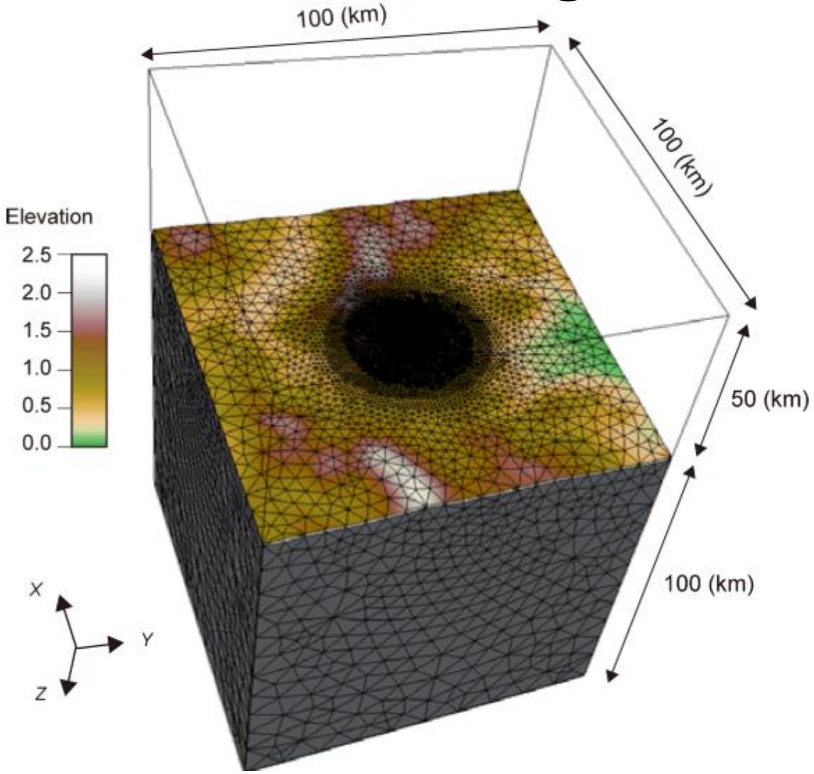

Usui *et al*. (2017, *GJI*)

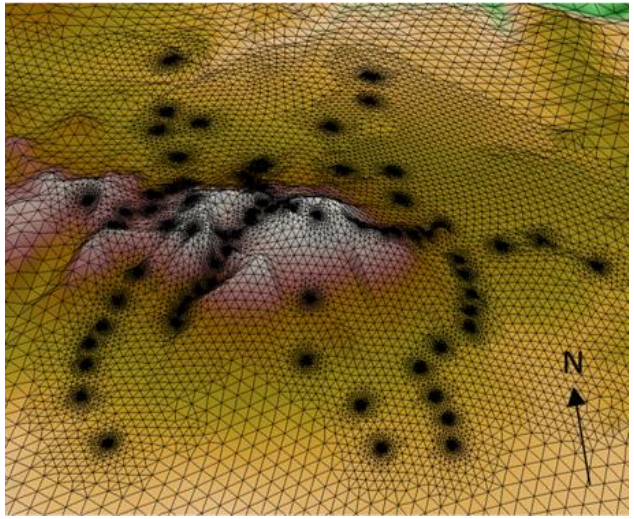

Resistivity structure across the summit of Asama volcano

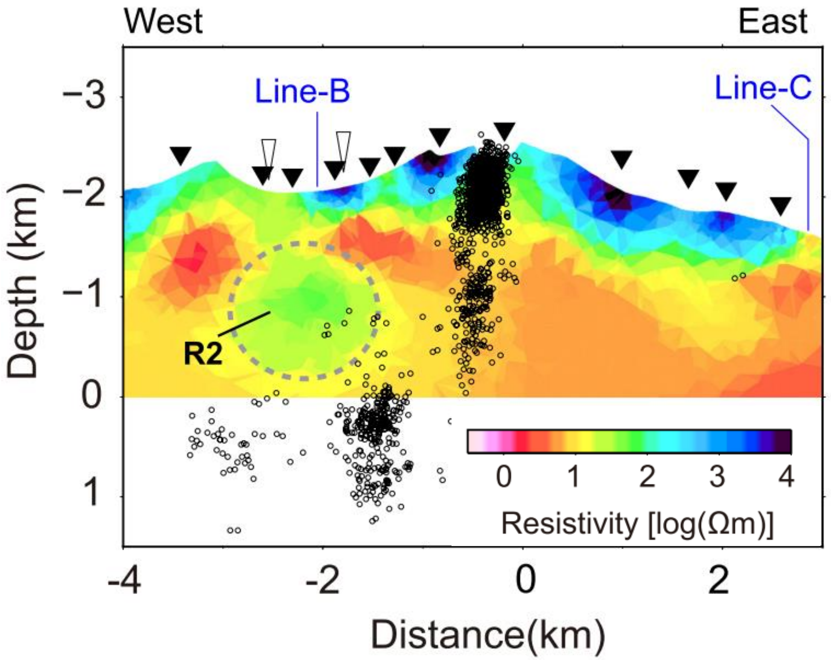

- Usui (2015, *GJI*) developed a 3-D MT inversion method using the tetrahedral element.
- Usui *et al.* (2017, *GJI*) modified the inversion method to use the data-space Gauss-Newton method to speed up the inversion.
- Usui *et al.* (2017, *GJI*) applied the developed inversion code to the MT data measured on Asama volcano, Japan.

3-D marine MT inversion using tetrahedral mesh

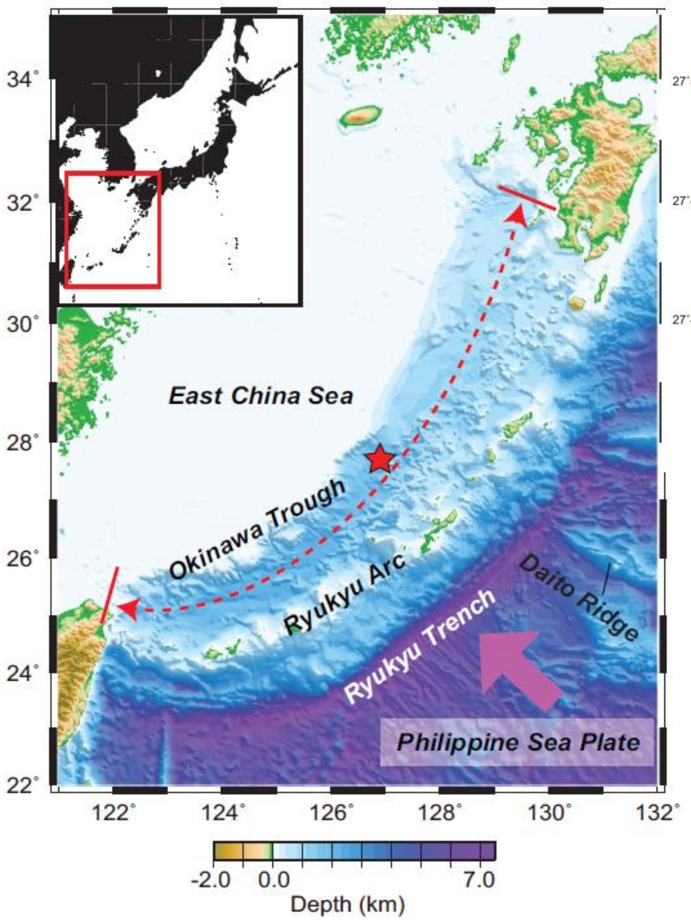

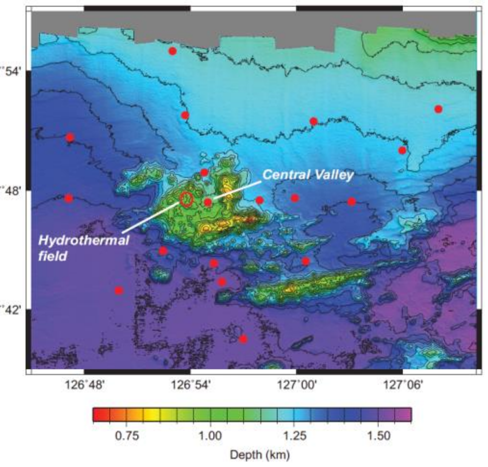

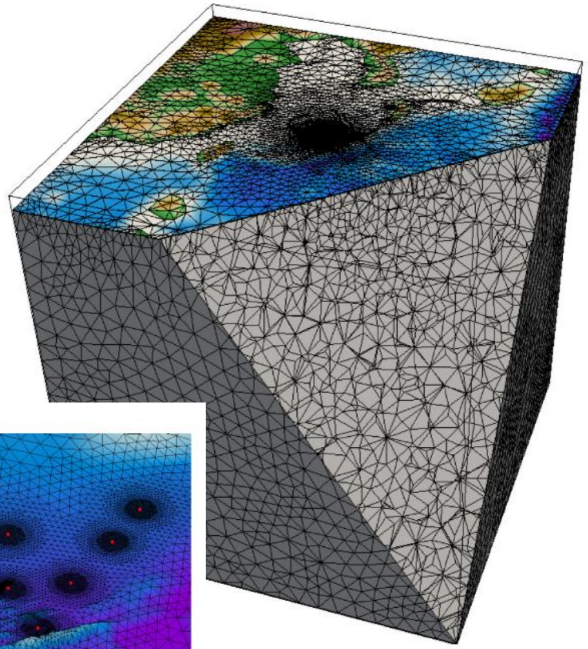

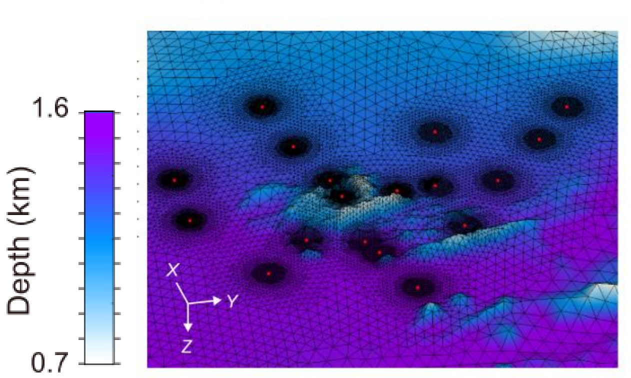

Resistivity structure across the summit of the Iheya North Knoll, middle Okinawa Trough

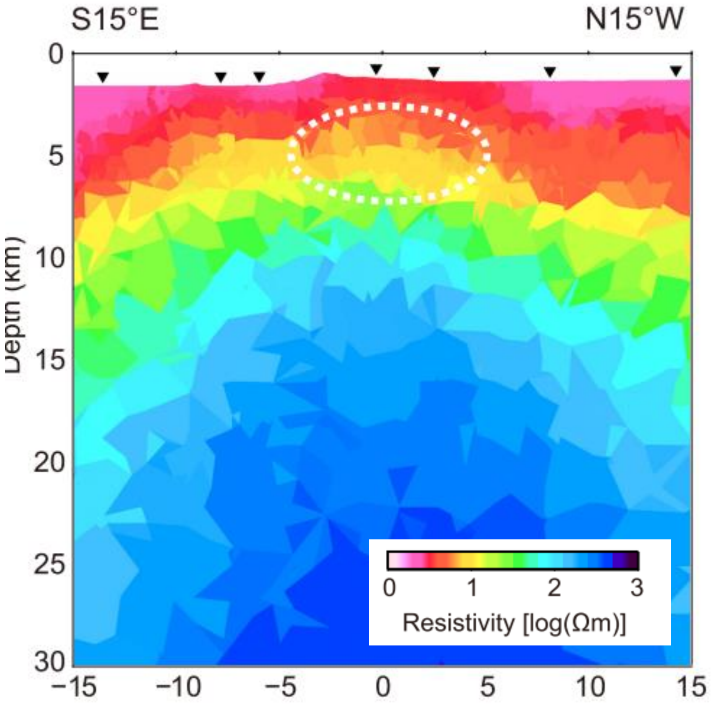

Usui *et al*. (2018, *GJI*)

- Usui *et al*. (2018, *GJI*) confirmed that the developed can be applied to marine MT data.
- Usui *et al*. (2018, *GJI*) applied the developed code to the MT data measured on the Iheya North Knoll (middle Okinawa Trough), where a lot of active hydrothermal mounds are situated.

3-D MT inversion using tetrahedral mesh

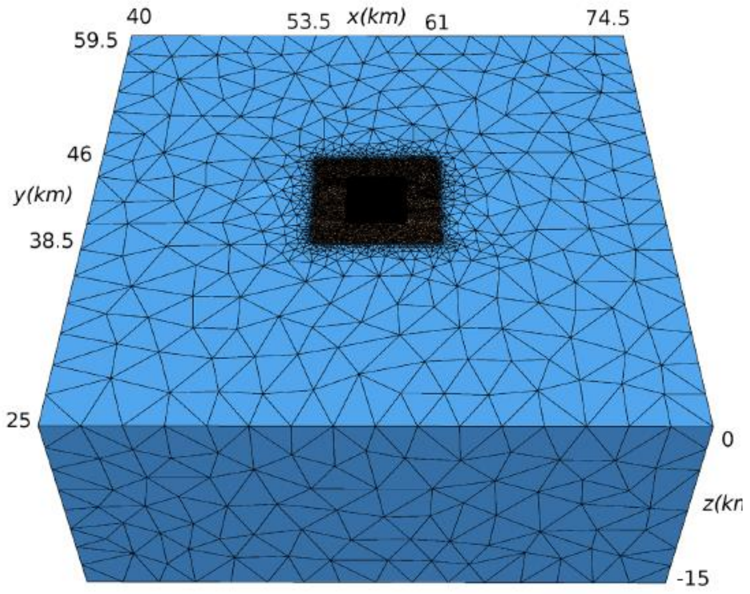

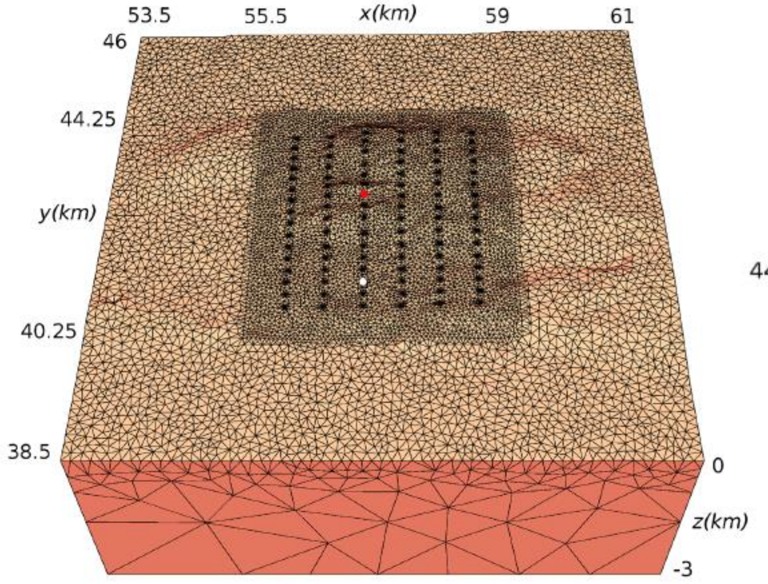

True model

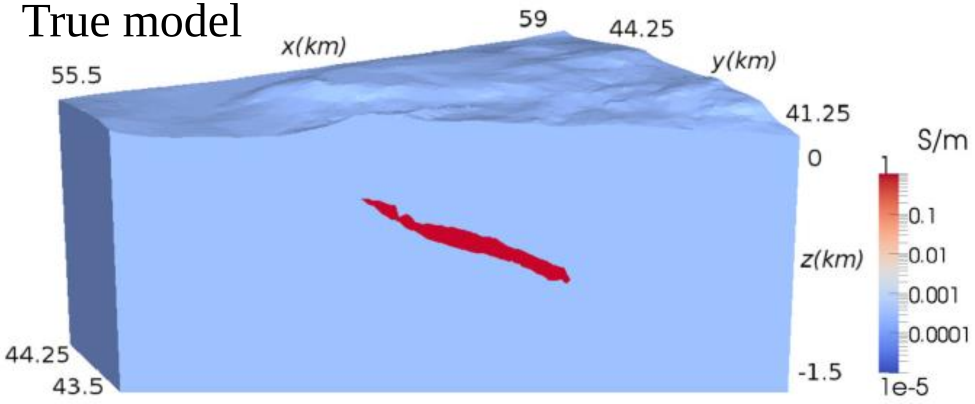

Inversion result

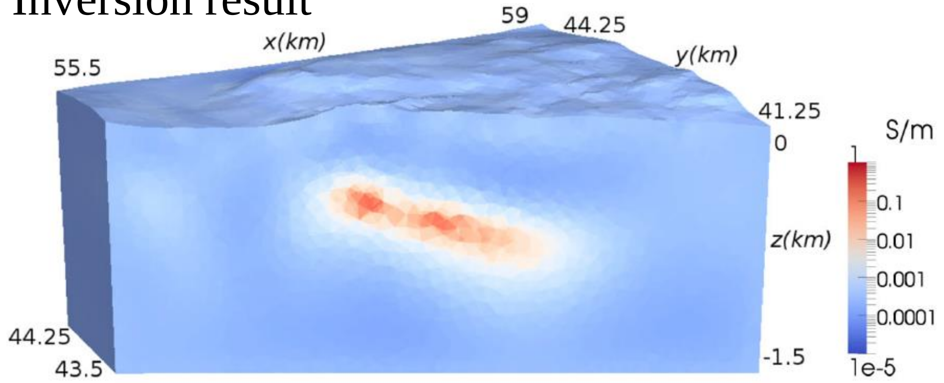

Jahandari & Farquharson (2017, *GJI*)

- Jahandari & Farquharson (2017, *GJI*) developed another 3-D MT inversion using tetrahedral element.
- Jahandari & Farquharson (2017, *GJI*) confirmed the effectiveness of the code by synthetic inversion analyses using the COMMEMI 3D-1A model (Zhdanov *et al.* 1997, *J. appl. Geophys.*) and a model of the Eastern Deeps zone sulphide deposit in Voisey's Bay, Labrador.

Hexahedral mesh vs Tetrahedral mesh

- I think the FEM using a non-conforming hexahedral mesh or a tetrahedral mesh is one of the best way to incorporate topography and bathymetry at present.
- Both non-conforming hexahedral mesh and tetrahedral mesh enable us to accurately include undulations of the earth's surface in the MT modeling.
- Both of them enable us to make locally refined mesh,
- The pros and cons below is only my personal view.

If hexahedral mesh is used, block-shaped approximation of the coastline is usually necessary

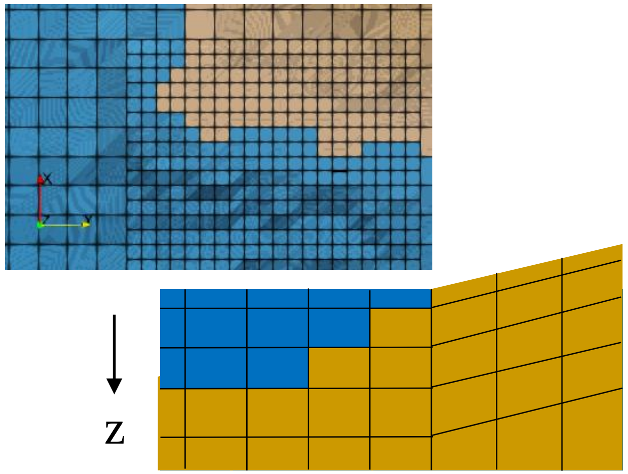

Coastline cannot be as accurately represented as by tetrahedral mesh.

Representation accuracy of coastline

Easiness of meshing

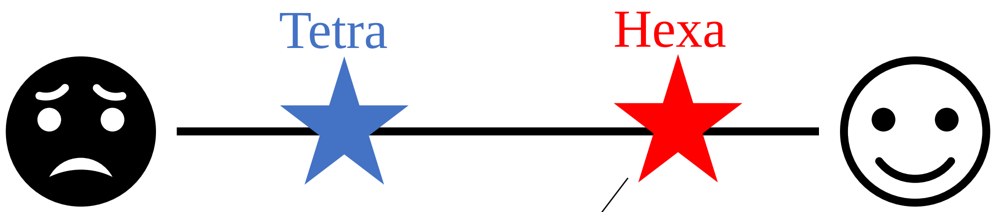

Making process of a hexahedral mesh is much easier than that of a tetrahedral mesh.

Other approaches with a good potential to incorporate topography/bathymetry (1)

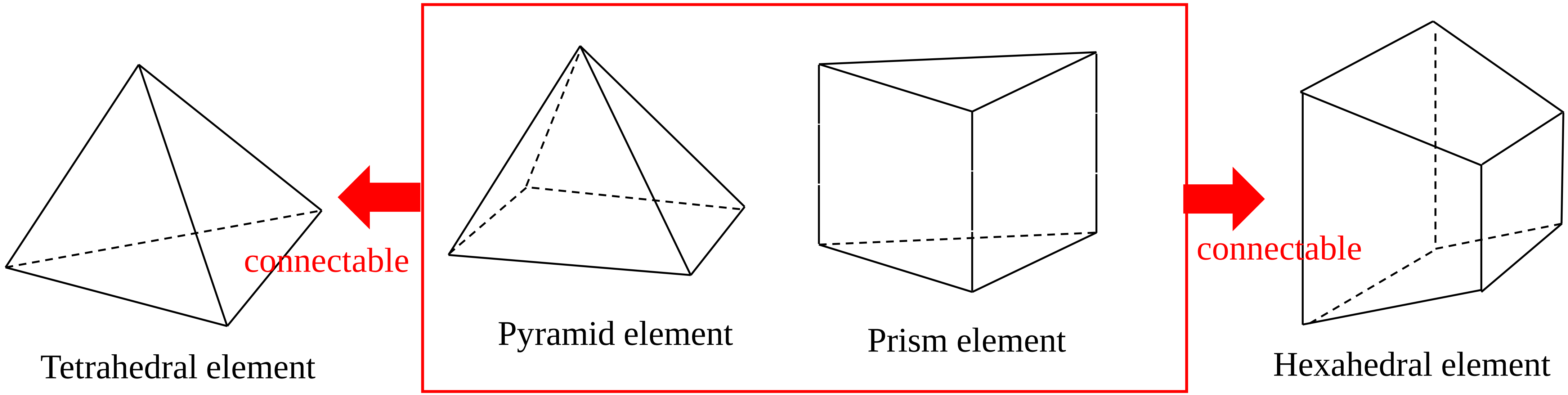

- Formulations for pyramid-shaped and prism-shaped elements have been proposed in the FEM.
- These element can be used to connect tetrahedral element and hexahedral element.
- By combining several types of elements, maybe, we can overcome disadvantages of each element.

For example, hexahedral elements are used for the whole area except for near coastlines, and other types of elements are used to represent coastlines accurately.

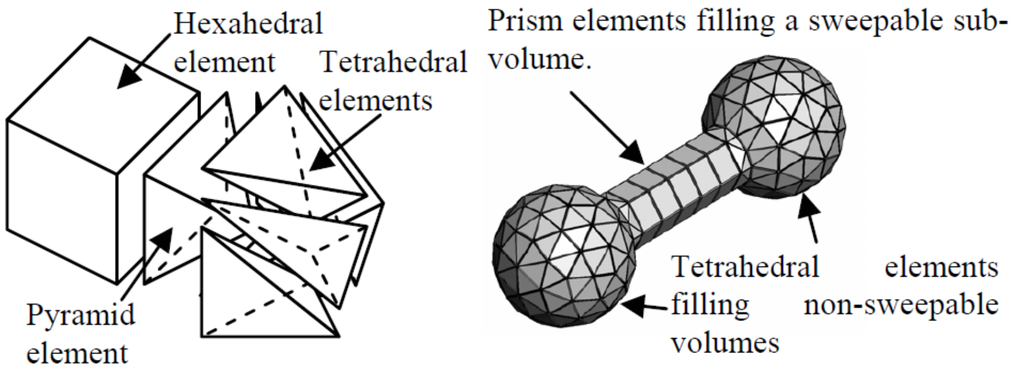

Yamakawa & Shimada (2008)

Other approaches with a good potential to incorporate topography/bathymetry (2)

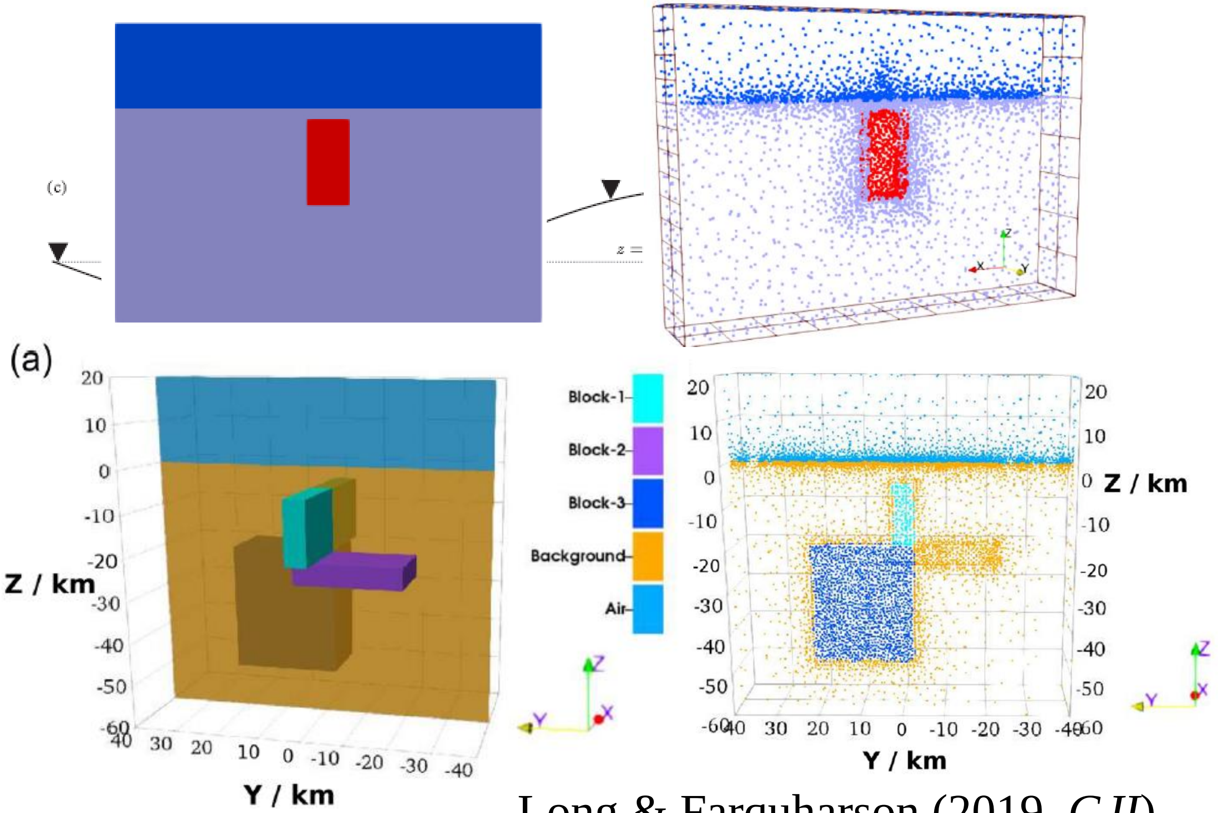

Long & Farquharson (2019, *GJI*)

Inversion result by a 2-D FDM code

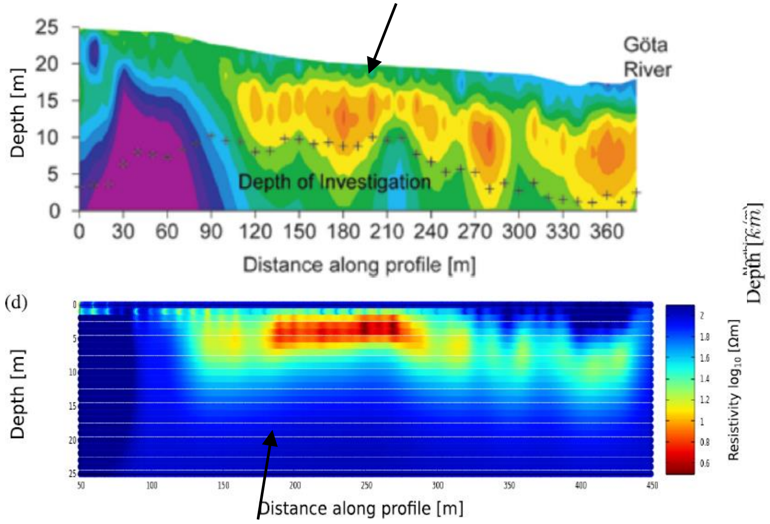

Meshless inversion result

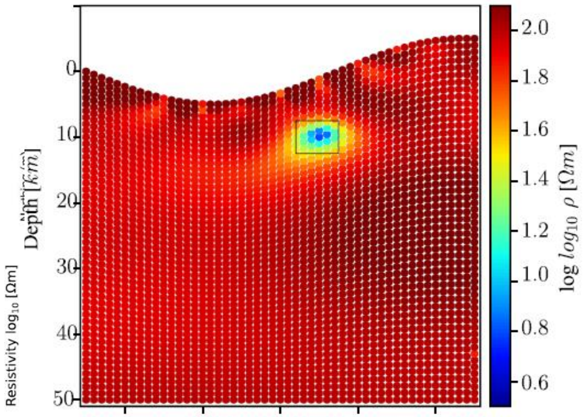

Wittke & Tezkan (2021, *GJI*)

- Long & Farquharson (2019, *GJI*) developed a 3-D MT forward calculation method using a mesh-free approach.
- Wittke & Tezkan (2021, *GJI*) developed a 2-D MT inversion method using a mesh-free approach.
- If 3-D MT inversion method based on a mesh-free approach is developed, mesh-free method will be used as another effective approach to incorporate topography and/or bathymetry in 3-D MT inversion.

Agenda

1. Influences of topography and bathymetry on MT response functions
2. Review of the methods to incorporate topography and bathymetry in 3-D MT modeling
3. Brief introduction of 3-D MT inversion code FEMTIC

FEMTIC code on GitHub

- FEMTIC code (Usui 2015; Usui *et al*. 2017; Usui *et al*. 2018) is available from GitHub.
- This code was made using object-oriented programming with C++.

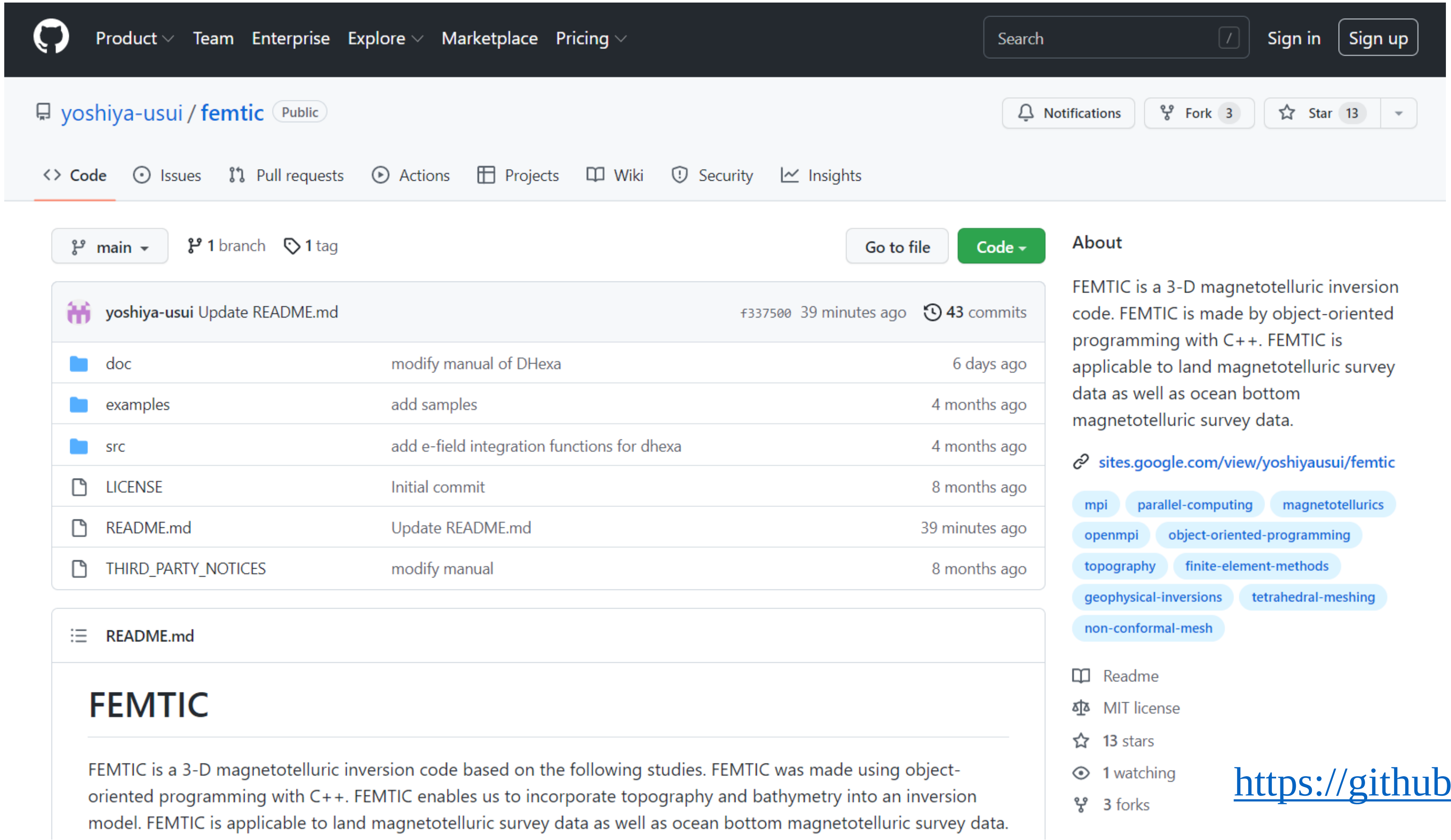

https://github.com/yoshiya-usui/femtic

Functional overview

Mesh type: Tetrahedral mesh / Non-conforming deformed hexahedral mesh / Hexahedral brick mesh

Model parameter: Subsurface electrical resistivity / Distortion matrix of galvanic distortion

Data type: Impedance tensor / Vertical magnetic transfer function / Inter-station horizontal magnetic transfer function / Phase tensor / Apparent resistivity & Phase.

Inversion algorithm: Model-space Gauss-Newton method / Data-space Gauss-Newton method

Parallel computation: Multiple processes parallel computation with MPI / Multiple threads parallel computation with OpenMP / MPI & OpenMP hybrid parallel computation

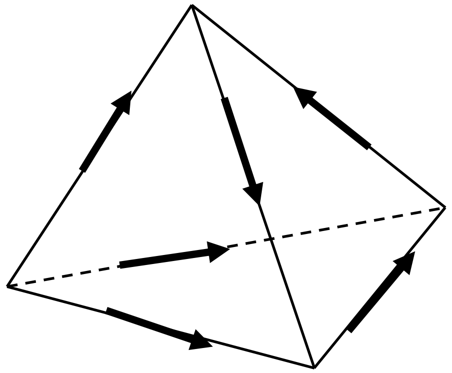

Tetrahedral element

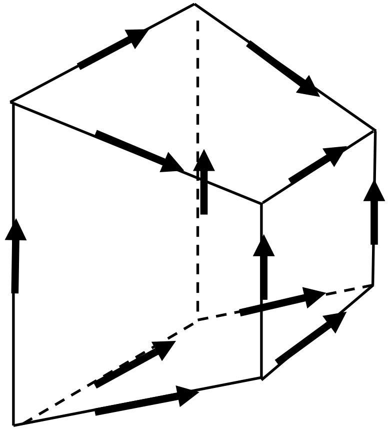

Hexahedral element

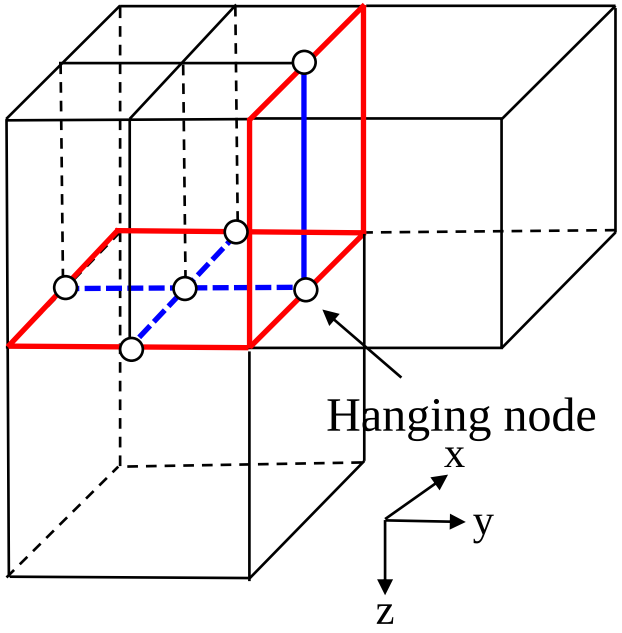

- I basically followed the approach of Grayver & Bürg (2014, *GJI*) for the treatment of non-conforming mesh.
- However, in FEMTIC, division numbers of only horizontal edges can be doubled.

Forward calculation results for a trapezoidal hill

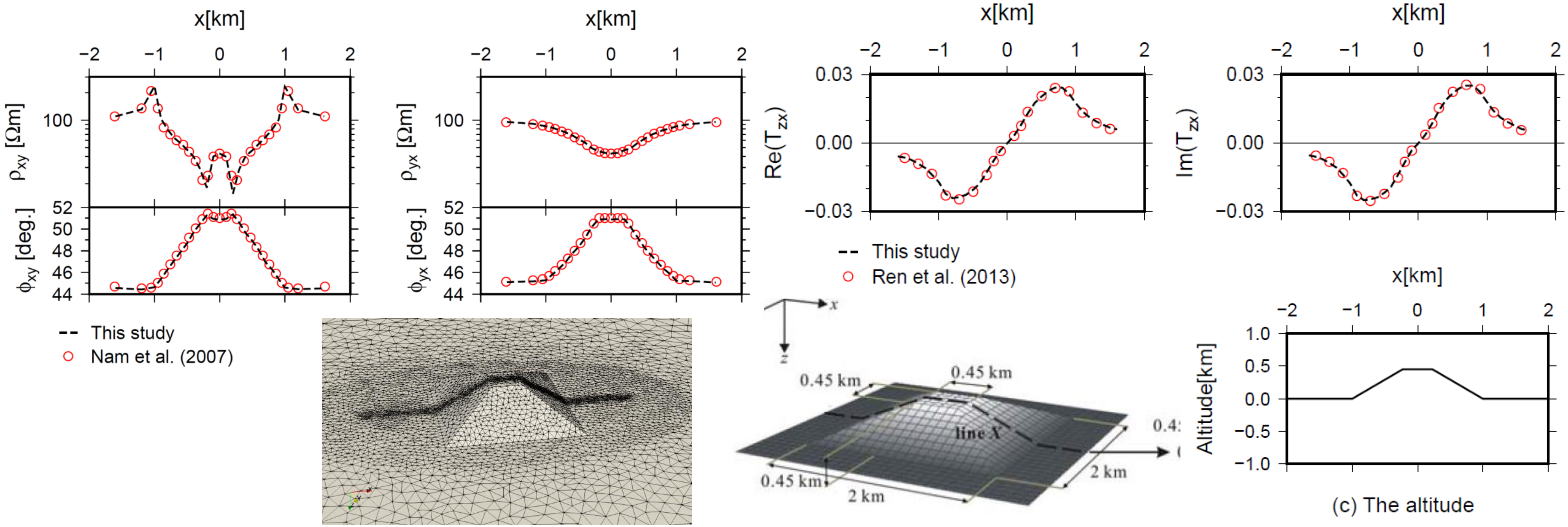

- ➢ I calculated the apparent resistivity, phase, and tipper for the trapezoidal hill model of Nam *et al*. (2007, *Geophys. Prospect.*) using a tetrahedral mesh.
- ➢ The calculated response functions were very close to the results of the previous studies (Nam *et al*. 2007, *Geophys. Prospect.;* Ren *et al.* 2013, *GJI*)

Forward calculation results for a sinusoidal seafloor

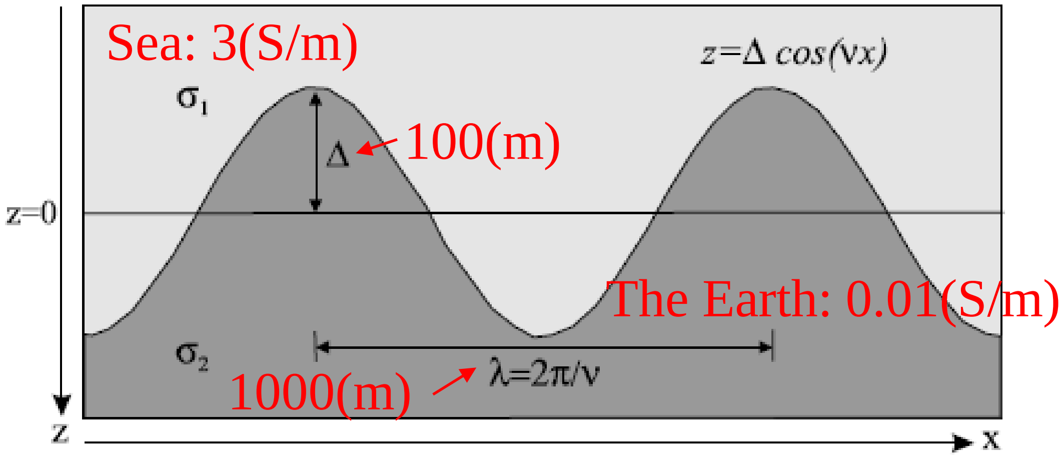

Schwalenberg & Edwards (2004, *GJI*)

Mesh of the sea and the subsurface

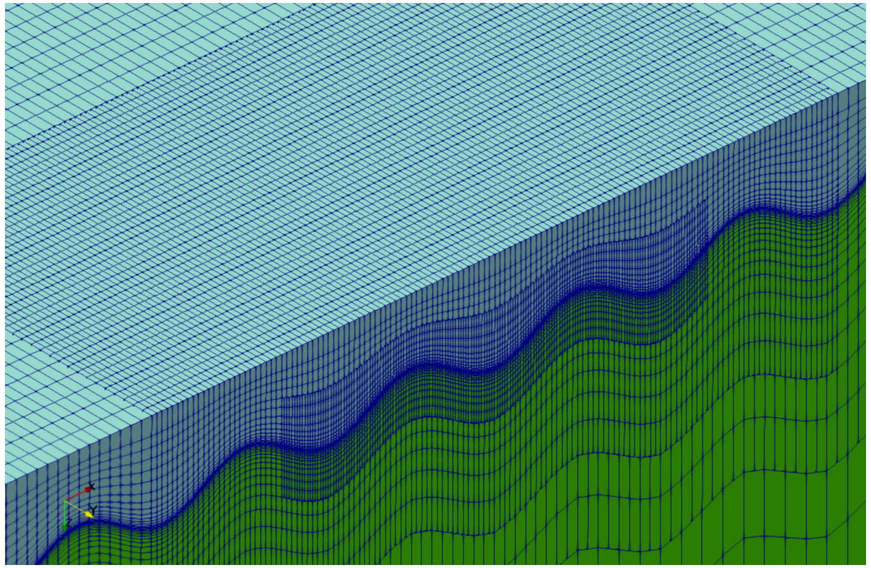

Mesh of the subsurface

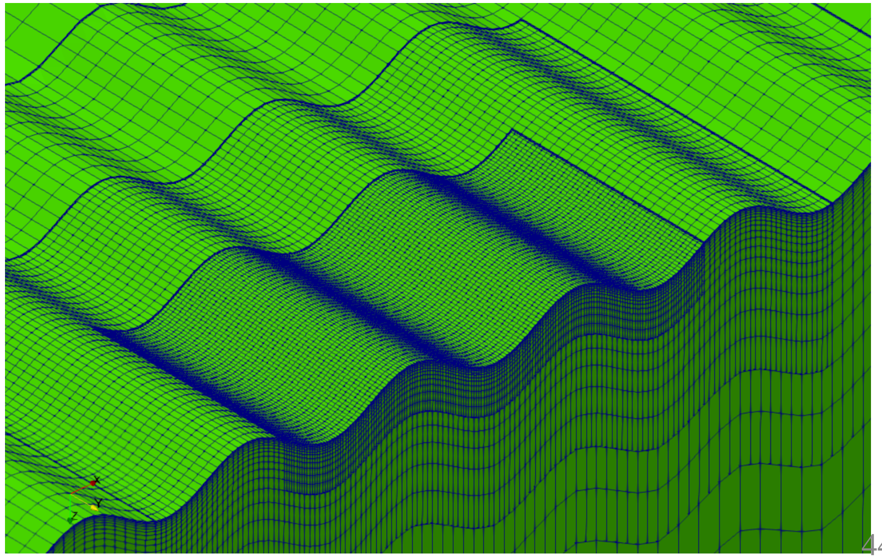

- I calculated the apparent resistivity, phase, and tipper for a sinusoidal 2-D seafloor model.
- I modeled a sinusoidal seafloor using a 3-D non-conforming deformed hexahedral mesh.

Forward calculation results for a sinusoidal seafloor

Bathymetry

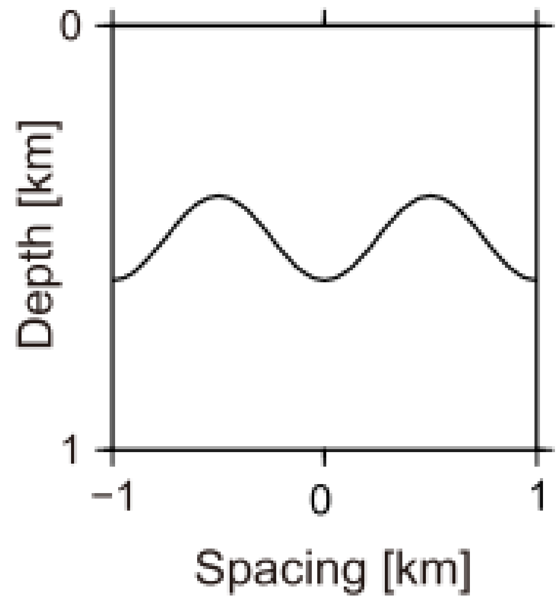

Apparent resistivity (TM-mode)

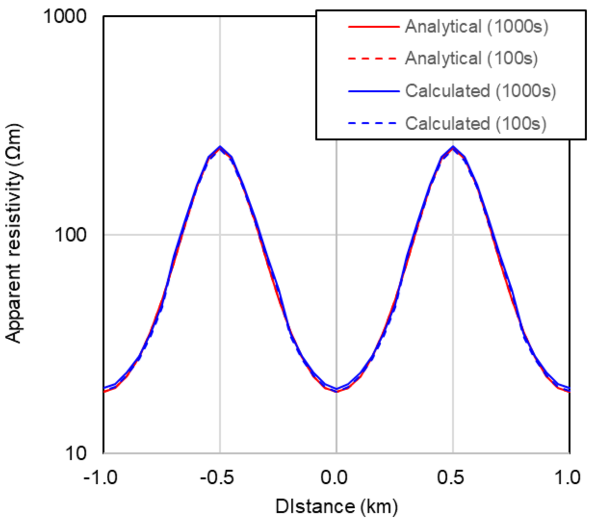

Phase (TM-mode)

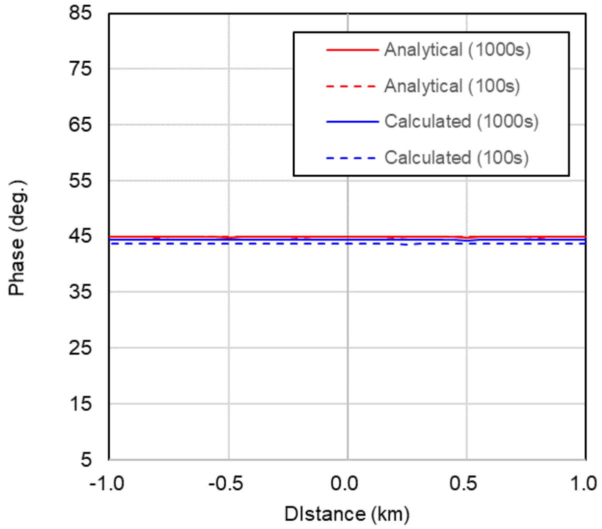

Tipper (Real part)

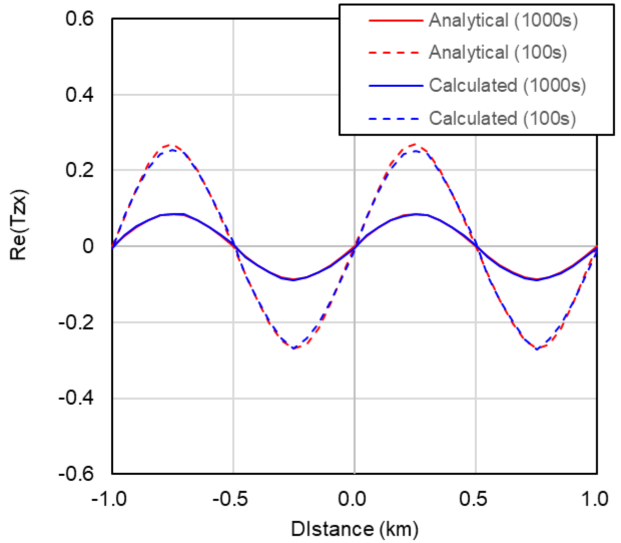

Apparent resistivity (TE-mode)

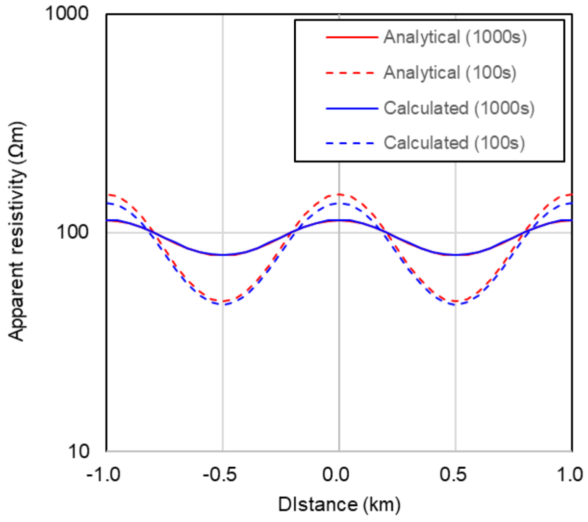

Phase (TE-mode)

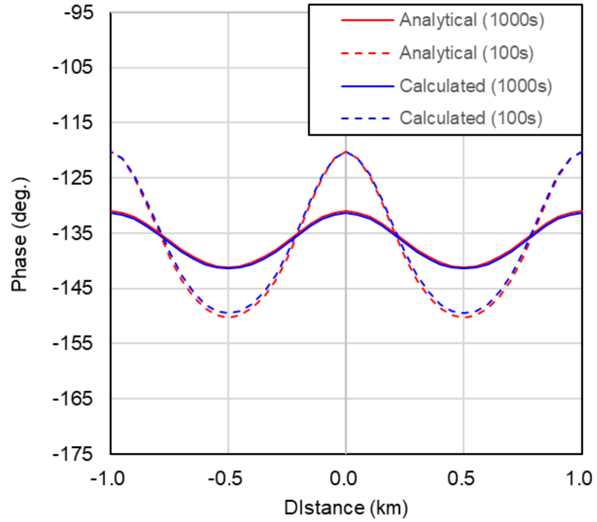

Tipper (Imaginary part)

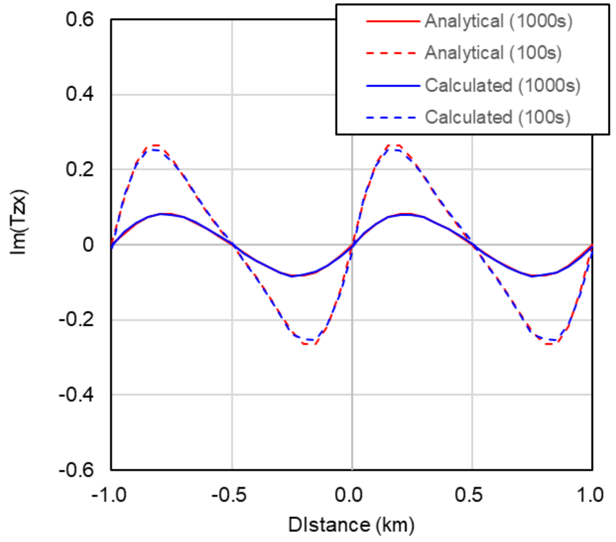

The calculated response functions were very close to analytical solutions.

END